

**PROJECT 1: MICRORNA REGULATION OF THE  
PROTO-ONCOGENE PBF**

and

**PROJECT 2: RECOGNITION OF PREVIOUSLY  
UNDESCRIBED RING DOMAIN RESIDUES  
REQUIRED FOR BRCA1:BARD1 AND RING1B:BMI1  
UBIQUITIN LIGASE ACTIVITY**

by

ALICE FLETCHER

This project is submitted in partial fulfilment of the requirements for the award  
of the MRes Biomedical Research 2013/2014.



UNIVERSITY OF  
BIRMINGHAM

College of Medical and Dental Sciences

University of Birmingham

May 2014

UNIVERSITY OF  
BIRMINGHAM

**University of Birmingham Research Archive**

**e-theses repository**

This unpublished thesis/dissertation is copyright of the author and/or third parties. The intellectual property rights of the author or third parties in respect of this work are as defined by The Copyright Designs and Patents Act 1988 or as modified by any successor legislation.

Any use made of information contained in this thesis/dissertation must be in accordance with that legislation and must be properly acknowledged. Further distribution or reproduction in any format is prohibited without the permission of the copyright holder.

**MICRORNA REGULATION OF THE  
PROTO-ONCOGENE PBF**

by

ALICE FLETCHER

This project is submitted in partial fulfilment of the requirements for the award  
of the MRes Biomedical Research 2013/2014.

## ABSTRACT

In thyroid cancers there have been independent observations of the overexpression of a relatively uncharacterised proto-oncogene, known as PBF, as well as the deregulation of microRNAs. However, little remains known about how PBF is regulated although, a recent investigation has identified miR-122 to have the ability to regulate PBF in hepatitis B and liver cancer.

Therefore, the aims of this investigation were to identify whether a selection of microRNAs can regulate PBF, altering its mRNA expression and protein levels. This was achieved by selecting microRNAs predicted to target PBF, transfecting SW1736 thyroid carcinoma and MCF7 breast carcinoma cell lines with microRNA mimics of these, then measuring PBF expression by qRT-PCR and Western blotting.

The most striking result indicated that hsa-miR-122-5p caused a significant decrease in PBF protein levels cells despite no change in PBF mRNA expression. Furthermore, hsa-miR-124-3p and hsa-miR-506-3p also negatively regulated PBF mRNA expression and protein levels; highlighting microRNAs do have the ability to regulate PBF. Due to the emerging importance of microRNAs as biomarkers and therapeutics the identification of specific microRNAs that play a role in thyroid cancer may bear clinical relevance although, these initial findings need to be confirmed and extended for a more stringent investigation.

## **ACKNOWLEDGEMENTS**

Having thoroughly enjoyed my experience within the McCabe group I would firstly like to thank Professor Chris McCabe for giving me the opportunity to work on this project as well as his encouragement and support throughout, as without him this investigation would not have been possible.

I would also like to thank all the other members of the McCabe group; Dr Vicki Smith, Dr Rachel Watkins, Dr Martin Read, Bhav Modasia, Vikki Poole, Waraporn Imruetaicharoenchoke and Teresa Gagliano who have not only helped me throughout but also created a friendly working environment enhancing my lab experience.

# CONTENTS

<b>1. Introduction</b> .....	1
<b>1.1. Thyroid Cancer</b> .....	1
<b>1.2. Pituitary Tumor Transforming Gene (PTTG) Binding Factor (PBF)</b> .....	2
1.2.1. PBF Expression in Thyroid Cancer.....	3
<b>1.3. MicroRNAs</b> .....	4
1.3.1. MicroRNAs in Thyroid Cancer.....	8
<b>1.4. Aims</b> .....	8
<b>2. Materials &amp; Methods</b> .....	10
<b>2.1. MicroRNA Selection</b> .....	10
<b>2.2. Cell Lines</b> .....	10
2.2.1. Transfection.....	10
<b>2.3. RNA Analysis</b> .....	11
2.3.1. RNA Isolation.....	11
2.3.2. Reverse Transcription PCR (RT-PCR).....	11
2.3.3. Quantitative Real-Time PCR (qRT-PCR).....	12
2.3.4. Statistics.....	12
<b>2.4. Protein Analysis</b> .....	13
2.4.1. Protein Harvest.....	13
2.4.2. Western Blotting.....	13
2.4.3. Statistics.....	14
<b>3. Results</b> .....	15
<b>3.1. MicroRNAs Predicted to Target PBF</b> .....	15
3.1.1. hsa-miR-1.....	15
3.1.2. hsa-miR-122-5p.....	15

3.1.3. hsa-miR-124-3p.....	16
3.1.4. hsa-miR-193b-5p.....	16
3.1.5. hsa-miR-506-3p.....	17
<b>3.2. Effect on PBF mRNA Expression Following MicroRNA Mimic Transfections.....</b>	<b>18</b>
3.2.1. Effect on PBF mRNA Expression Following MicroRNA Mimic Transfections in SW1736 Cells.....	18
3.2.2. Effect on PBF mRNA Expression Following MicroRNA Mimic Transfections in MCF7 Cells.....	23
<b>3.3. Effect on PBF Protein Levels Following MicroRNA Mimic Transfections.....</b>	<b>25</b>
3.3.1. Effect on PBF Protein Levels Following MicroRNA Mimic Transfections in SW1736.....	25
3.3.2. Effect on PBF Protein Levels Following MicroRNA Mimic Transfections in MCF7 Cells.....	33
<b>4. Discussion.....</b>	<b>35</b>
<b>4.1. hsa-miR-122-5p Decreased PBF Protein Levels.....</b>	<b>35</b>
<b>4.2. hsa-miR-124-3p and hsa-miR-506-3p Decreased PBF mRNA Expression and Protein Levels.....</b>	<b>37</b>
<b>4.3. Limitations.....</b>	<b>38</b>
<b>4.4. Future Research.....</b>	<b>40</b>
<b>4.5. Conclusion.....</b>	<b>42</b>
<b>5. References.....</b>	<b>43</b>
<b>6. Appendix.....</b>	<b>47</b>





# 1. INTRODUCTION

## 1.1. Thyroid Cancer

Thyroid cancers are a rare type of cancer (<http://www.cancerresearchuk.org/cancer-help/type/thyroid-cancer/about/thyroid-cancer-risks-and-causes>) divided into four main groups dependent on the origin of the cancer cells within the thyroid gland, which is composed of parafollicular and follicular cells. Medullary thyroid carcinomas (MTC) are derived from parafollicular cells and are quite rare whereas tumours derived from follicular cells are more common and are divided into subtypes classified as; differentiated and undifferentiated carcinomas (Dvořáková, S., et al., 2014). Differentiated carcinomas include papillary thyroid carcinomas (PTC) and follicular thyroid carcinomas (FTC), which are slow growing and usually curable (Mazzaferri, E.L. and Kloos, R.T., 2001). The most common treatment for these is surgery followed by the use of radioiodine, which exploits the ability of the thyroid to take up iodine via the sodium iodide symporter (NIS) (Smith, V.E., et al., 2013). In comparison, undifferentiated carcinomas - known as anaplastic thyroid carcinomas (ATC) - are extremely lethal as they are aggressive and metastasise, resulting in a median patient survival of less than six months (Lim, S.M., et al., 2012).

There are multiple risk factors for thyroid cancer, including; a family history of thyroid cancer, an enlarged goitre and radiation exposure as well as being female, which results in thyroid cancer being two to three times more common in women compared to men (<http://www.cancerresearchuk.org/cancer-help/type/thyroid-cancer/about/thyroid-cancer-risks-and-causes>). At the molecular level, it has been described that the genetics of thyroid cancer also act as risk factors with genetic alterations described to be apparent in approximately 75% of cases (Bhaijee, F. and Nikiforov, Y.E., 2011, Read, M.L., et al., 2014).

Furthermore, the overexpression of certain proteins has also been observed in thyroid cancers, including overexpression of the proto-oncogene; pituitary tumor transforming gene 1 (PTTG1) binding factor (PBF), also known as PTTG1 interacting protein (PTTG1IP).

## 1.2. Pituitary Tumor Transforming Gene (PTTG) Binding Factor (PBF)

PBF is a 180 residue long protein (Read, M.L., et al., 2011) with a molecular weight of approximately 25kDa (Smith V. and McCabe, C., 2008), which was first identified due to its interaction with PTTG1 via PBF's C-terminus (Figure 1) (Chien, W. and Pei, L., 2000). This interaction between PTTG1 and PBF was described to induce the translocation of PTTG1 from the cytoplasm into the nucleus (Stratford, A.L., et al., 2005) driving tumourigenesis (Smith, V.E., et al., 2011). As PBF has no significant homology to any other human protein (Read, M.L., et al., 2011), it has been described as a 'relatively uncharacterised protein' however, since it was recognised that PBF has a transforming ability of its own both *in vitro* and *in vivo* PBF has subsequently been defined as a proto-oncogene in its own right (Smith, V.E., et al., 2011), gaining increasing interest.



### Figure 1: PBF functional domains

Schematic of signals and domains on PBF, responsible for its cellular location, as well as the PTTG1 binding site, found at the C-terminus.

Smith V. and McCabe C., 2008. PTTG1IP (Pituitary Tumor-Transforming 1 Interacting Protein). Atlas of Genetics and Cytogenetics in Oncology and Haematology. (Image from: <http://AtlasGeneticsOncology.org/Genes/PTTG1IPID41944ch21q22.html> accessed on 27/12/13).

### *1.2.1. PBF Expression in Thyroid Cancer*

The aforementioned overexpression of the proto-oncogene PBF within thyroid cancers, as well as breast cancers, is observed at both the mRNA expression and protein level, compared to the standard ubiquitous expression in normal thyroid tissue (Stratford, A.L., et al., 2005). This overexpression has been independently associated with a poor prognosis and lower disease-specific survival in thyroid cancers (Read, M.L., et al., 2014), likely due to the correlation with; distant metastases at diagnosis, tumour multicentricity and locoregional recurrence (Hsueh, C., et al., 2013). Subsequently, this has resulted in PBF being described as a promising prognostic marker within thyroid cancer (Hsueh, C., et al., 2013), which is of interest due to the recent incidences of thyroid cancer increasing faster than that of any other malignancy in both genders and all ethnic backgrounds (Tuttle, R.M., 2013).

Despite the precise role of PBF not being defined, investigations have begun to characterise PBF with respect to its roles in thyroid biology and tumourigenesis. One of the first functions of PBF defined with respect to thyroid cancer was its ability to act as a regulator of NIS. By preventing NIS function and expression at the plasma membrane PBF was consequently able to result in a repressed and insufficient radioiodine uptake during the treatment of differentiated thyroid cancers leading to a poor prognosis (Boelaert, K., et al., 2007). PBF has also been observed to interact with cortactin, a cytoplasmic protein involved in actin cytoskeleton rearrangement, thus facilitating cell migration and invasion (Sharma, N., et al., 2012), making it unsurprising that PBF overexpression correlates with metastases (Hsueh, C., et al., 2013). Furthermore, in transgenic mice models where PBF is overexpressed in the thyroid gland an upregulation of Akt and the TSH receptor have been observed, which are known regulators of thyroid follicular cell proliferation (Read, M.L., et al., 2011).

Most recently, PBF has been identified to be a regulator of the tumour suppressor p53 by specifically binding to p53 in thyroid cells and repressing transactivation of responsive promoters, as well as decreasing p53 stability via ubiquitination (Read, M.L., et al., 2014). This is an important finding as it has been well-documented that a disruption to p53 is observed in numerous cancers (Read, M.L., et al., 2014), highlighting the importance of regulating PBF due to the downstream impact it may have on tumourigenesis.

Despite an overexpression of PBF being observed in thyroid and breast cancer, very little remains known about what causes PBF overexpression. Previously, it has been described that PBF has oestrogen response elements (ERE) within its promoter region, with a correlation observed between the number of EREs and PBF expression in ER-positive breast tumours, resulting in oestrogen-stimulated cell invasion (Watkins, R.J., et al., 2010). Furthermore, it has been observed that hsa-miR-122 can regulate PBF in chronic hepatitis B (CHB) and hepatocellular carcinomas (HCC) (Li, C., et al., 2012).

### **1.3. MicroRNAs**

The observation of miR-122 regulating PBF is particularly interesting due to the increasing emergence of microRNAs being used as both biomarkers and therapeutics in cancer. Subsequently, recognition of the potential ability of microRNAs to regulate PBF contributed to the aims and hypotheses within this investigation, whereby the deregulation of specific microRNAs is hypothesised to result in PBF overexpression, as observed in thyroid cancer.

MicroRNAs are short (21-25 nucleotides in length) non-coding RNAs that negatively regulate gene expression at the post-transcriptional level by binding to the 3' UTR of their target mRNAs and preventing protein production (Cannell, I.G., et al., 2008) (Figure 2). As microRNAs account for 1-5% of the human genome (MacFarlane, L.A. and Murphy, P.R.,

2010) and each microRNA has approximately 200 mRNA targets (Carther, R.W., 2006) they are able to target more than 60% of human protein-coding genes (Friedman, R.C., et al., 2009).

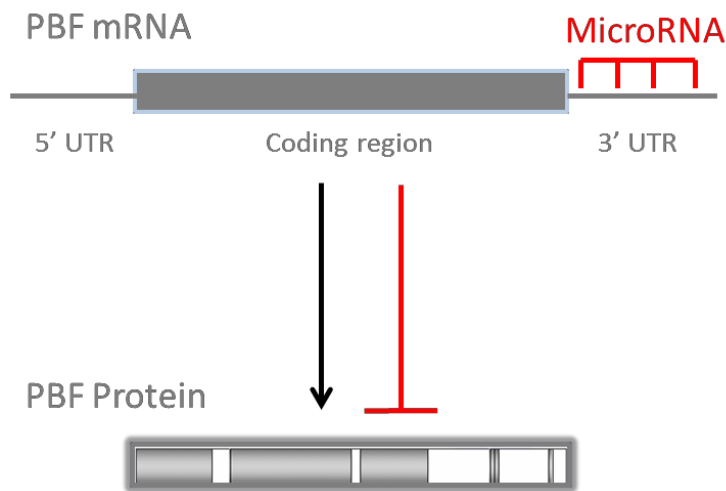


**Figure 2: MicroRNA Targeting of mRNA**

Schematic of a microRNA (red) targeting the 3' UTR of its mRNA target (grey), in this case PBF. This results in the prevention of translation and thus protein expression.

Before targeting their mRNA target, microRNAs must be transcribed and processed from their own genes. In animals, microRNAs are transcribed by RNA polymerase II in the nucleus as a long polycistronic primary transcript with a hairpin (Lee, Y., et al., 2004) (Figure 3). Following transcription, the upper part of the hairpin is excised by Drosha, an RNase III enzyme in the nucleus, to give a 65 nucleotide intermediate known as pre-microRNA (Figure 3). Exportin-5 then facilitates the export of pre-microRNAs from the nucleus into the cytoplasm (Yi, R. et al., 2003) where Dicer, another RNase III enzyme, removes the hairpin loop to give a RNA duplex (Cai, X., et al., 2004) (Figure 3). This duplex is then assembled into a protein complex known as the RNA-induced silencing complex (RISC), which contains Argonaute proteins (Ago (1-4)) at its centre used to separate the RNA duplex strands (Kawamata, T., et al., 2011). Subsequently, one strand of the duplex is degraded and the other strand remains as a mature microRNA guide strand (Figure 3), as determined by the internal stability of the duplex ends with a less stable 5' end resulting in strand survival (Lee, Y., et

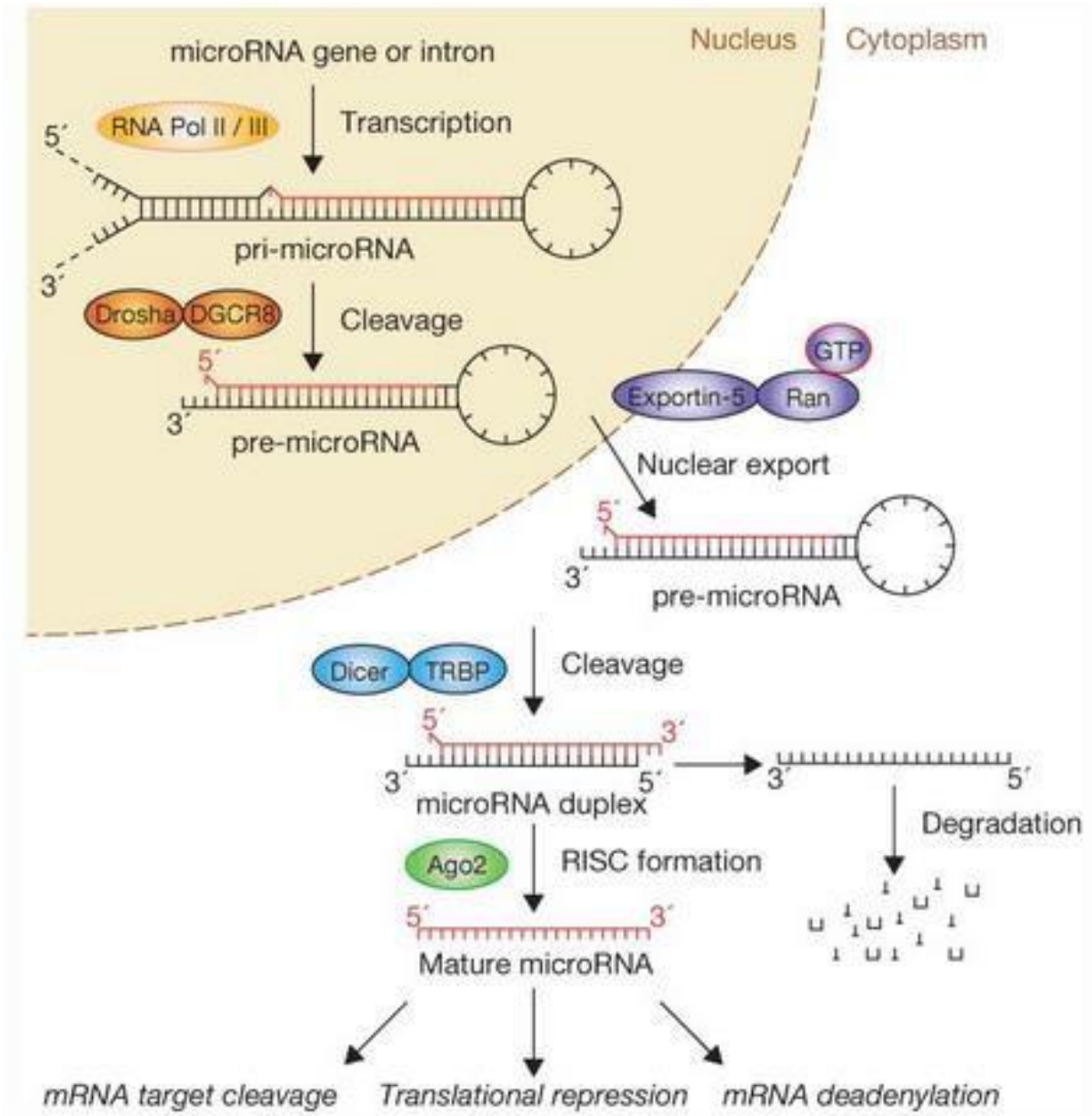


**Figure 3: Pathway of microRNA processing**

Pathway of microRNA processing starting from the long primary transcript (pri-microRNA) in the nucleus, which is cleaved by Drosha to give pre-microRNA. Exportin-5 along with Ran-GTP export pre-microRNA from the nucleus to the cytoplasm where Dicer cleaves the hairpin loop off to give the mature microRNA. The functional strand of the mature microRNA is then loaded onto Ago2 to form the RISC while the other strand gets degraded. RISC is then guided to its targets to cause mRNA target cleavage, translational repression or mRNA deadenylation. (Image from: Winter, J., et al., 2009. The Linear Canonical Pathway of MicroRNA Processing. Nature Cell Biology, 11, pp.228-234).

al., 2004). These processing steps ensure microRNA authenticity (Kawamata, T., et al., 2011) and guarantee the microRNA guide strand targets and binds the RISC to the correct mRNA target. This binding takes place via Watson-Crick base pairing, with a full-match base pairing between the seed region (residues 2-8 at the microRNA 5' end) and 3' UTR of the mRNA target, followed by a bulge region and then a region of partial complementarity (Ricci, E.P., et al., 2011).

Upon successful targeting of the microRNA, protein production is prevented by one of three methods; 1) slicer-dependent mRNA degradation, 2) slicer-independent translational repression or 3) mRNA degradation and translational repression in P-bodies (MacFarlane, L.A. and Murphy, P.R., 2010). Slicer-dependent mRNA degradation is where mRNA cleavage is catalysed by Ago2 in the RISC followed by the subsequent degradation of the mRNA products, which requires de-adenylation of the mRNA to remove the poly(A) tail making this an irreversible process (MacFarlane, L.A. and Murphy, P.R., 2010). In comparison, slicer-independent translational repression is due to the microRNA being bound to its mRNA target and physically preventing translation taking place. Although the exact mechanism remains unknown, it is known that Ago2 in the RISC has a cap-binding-like-motif making the 5' cap of the target mRNA important for translational repression (Cannell, I.G., et al., 2008). However, once this repression is relieved the mRNA can be translated again making this a reversible process (MacFarlane, L.A. and Murphy, P.R., 2010). Finally, the third method microRNAs use to repress protein expression of their target mRNAs is; mRNA degradation and translational repression within P-bodies (Liu, J., et al., 2005). P-bodies are cytoplasmic domains that contain enzymes and factors within specialised compartments required for mRNA decapping, deadenylation, RNA degradation and translational repression

allowing both slicer-dependent and slicer-independent silencing to take place inside (MacFarlane, L.A. and Murphy, P.R., 2010)

### *1.3.1. MicroRNAs in Thyroid Cancer*

MicroRNAs have been observed to be downregulated *in vivo* in mouse models of thyroid cancer (Visone, R., et al., 2007); highlighting the significance of microRNAs in thyroid tumourigenesis. Furthermore, microRNA expression has been observed to differ between normal and cancerous thyroid tissue, with 32% of microRNAs being upregulated and 38% being downregulated in thyroid tumours compared to normal tissues (Nikiforova, M.N., et al., 2009) and moreover, various microRNA signatures have been associated with each of the four groups of thyroid carcinomas; MTC, FTC, PTC and ATC (Abraham, D., et al., 2011, Jacques, C., et al., 2013, Visone, R., et al., 2007). Consequently, due to the observation of microRNA deregulation in thyroid cancers this has led to recognition of the use of microRNAs in both the diagnosis and prognosis of thyroid cancers (Leonardi, G.C., et al., 2012).

### **1.4. Aims**

The aim of this investigation was to determine whether specifically selected microRNAs can regulate PBF, due to independent observations of microRNA deregulation and PBF overexpression in thyroid cancers, as well as the recent observation of a microRNA, miR-122, targeting PBF in liver cancer. To determine the ability of microRNAs to target PBF, microRNA mimics of specifically selected microRNAs, alongside an anti-PBF siRNA as a control, were transfected into SW1736 and MCF7 cells, then PBF mRNA expression and PBF protein levels were assessed by qRT-PCR and Western blotting respectively.

It was hypothesised that PBF would be negatively regulated by the selected microRNAs and thus overexpression of these microRNAs by transfection would result in a decrease in PBF



mRNA expression and protein levels. Further investigations may determine whether there is a correlation between the downregulation of these microRNAs and PBF overexpression in thyroid cancer patient samples, which may consequently suggest clinical relevance due to the emergence of microRNAs as biomarkers and therapeutics in thyroid cancer.

## 2. MATERIALS & METHODS

### 2.1. MicroRNA Selection

Five microRNAs hypothesised to target PBF were selected by integrating results from the literature and prediction software, including; miRWalk (Dweep, H., et al., 2011), TargetScan (Friedman, R.C., et al., 2009), miRDB (Wang, X. and El Naga, I.M., 2008, Wang, X., 2008) and miRTarBase (Hsu, S.D., et al., 2010). In addition two controls were selected; a negative control siRNA, which has no homology to any known mammalian genes and anti-PBF siRNA, which directly targets PBF. These both identify thresholds for the effect of microRNA mimics, predicted to target PBF, to be measured against.

### 2.2. Cell Lines

The human BRAFV600E anaplastic thyroid carcinoma cell line (SW1736) and human estrogen receptor positive breast adenocarcinoma cell line (MCF7), both derived from Caucasians, were obtained from the Cell Lines Services (#300453) and European Collection of Cell Cultures (#86012803) respectively. They were maintained in RPMI 1640-L-Glutamine (Gibco) complete medium (10% FBS and 1% Penstrep) at 37°C and 5% CO<sub>2</sub> and sub-cultured frequently to ensure 80% maximum confluency.

#### 2.2.1. Transfection

24 hours before transfection, SW1736 and MCF7 cells were seeded at; 60,000 cells/well and 62,500 cells/well in 1ml RPMI 1640-L-Glutamine complete medium in 12-well plates for RNA analysis respectively and 150,000 cells/well and 125,000 cells/well in 2ml RPMI 1640-L-Glutamine complete medium in 6-well plates for protein analysis respectively. Transfection mixes were made by diluting the microRNA mimic (hsa-miR-1, hsa-miR-122-5p, hsa-miR-

124-3p, hsa-miR-193b-5p or hsa-miR-506-3p (Qiagen)), AllStars negative control siRNA (Qiagen) or anti-PBF siRNA (Life Technologies) in opti-MEM for a final concentration of 50nM. 12µl or 24µl HiPerfect transfection reagent (Qiagen)/well for 12-well or 6-well plates respectively was added to the transfection mixes, vortexed and incubated for 10 minutes according to the Qiagen protocol. Transfection mixes were then added in a dropwise manner to cells in a 12-well or 6-well plate. It is important to note that for RNA analysis, four replicates of each microRNA mimic and siRNA were transfected/experiment and for protein analysis one of each microRNA mimic and siRNA was transfected/experiment. Following transfection, cells were returned to 37°C and 5% CO<sub>2</sub> for 48 or 72 hours prior to RNA isolation or protein harvesting respectively.

## **2.3. RNA Analysis**

### *2.3.1. RNA Isolation*

48 hours after transfection, medium was aspirated from 12-well plates and cells were washed with PBS. PBS was aspirated and cells were lysed with 250µl TRI-Reagent (Sigma)/well at room temperature for 5 minutes. Lysates were transferred into Eppendorfs and stored at -80°C overnight. The next day the RNA isolation protocol was continued by adding 50µl chloroform (Sigma)/sample and incubating at room temperature for 5 minutes for phase isolation. Samples were centrifuged at 13,000xg and the colourless aqueous phase was transferred to a clean Eppendorf. To precipitate the RNA 125µl isopropanol (Sigma)/sample was added and incubated at room temperature for 20 minutes, followed by centrifugation at 13,000xg for 15 minutes. Supernatant was removed and the RNA pellet was washed with 250µl ethanol (VWR International)/sample for 5 minutes then left to air dry. Each sample was then re-suspended in 20µl nuclease free water (ProMega) and RNA concentration was determined by NanoDrop.

### *2.3.2. Reverse Transcription PCR (RT-PCR)*

Reactions mixtures for RT-PCR for each RNA sample contained: 0.5µg RNA in 5µl nuclease free water, 2µl MgCl<sub>2</sub>, 1µl RT 10x buffer, 1µl dNTP mixture (10mM), 0.25µl Recombinant RNasin, 0.25µl AMV RT and 0.5µl random primers (Reverse Transcription System, Promega). An AMV negative control reaction was made in the same way with a randomly selected duplicate 0.5µg RNA in 5µl nuclease free water, besides substituting AMV RT with nuclease free water. The Promega RT-PCR protocol was followed and reaction mixtures underwent the following RT-PCR programme: 42°C for 60 minutes, 95°C for 5 minutes, then 4°C for 3 minutes, following which cDNA samples were made to a total volume of 50µl with nuclease free water.

### *2.3.3. Quantitative Real-Time PCR (qRT-PCR)*

Within a PCR hood, reaction mixtures for qRT-PCR for each cDNA sample, including the AMV RT negative control, were added to a 96-well plate in duplicate for both PBF and 18S. Reaction mixtures contained: 2µl cDNA, 10µl 2x GoldStar TaqMan PCR mastermix (Eurogentec), 7µl nuclease free water and 1µl PTTG1IP TaqMan gene expression assay labelled with FAM dye (Life Technologies) or 1µl Eukaryotic 18S rRNA endogenous control labelled with VIC dye (Life Technologies) for PBF or 18S respectively. Control reactions were also added to the 96-well plate in duplicate for PBF and 18S, made exactly the same, besides substituting 2µl cDNA with nuclease free water. Following this, plates were sealed, centrifuged and underwent the following qRT-PCR programme: 50°C for 2 minutes for optimal enzyme activity, 95°C for 10 minutes to activate the AmpliTaq Gold and then for the PCR; 40 cycles of 95°C for 15 seconds and 60°C for 1 minute to denature, anneal and extend DNA.

#### 2.3.4. Statistics

7500 system software was used to analyse qRT-PCR data (Supplementary figures 1 and 2), with PBF mRNA expression normalised against 18S (CT values between 9 and 10) for each sample. qRT-PCR duplicates were then averaged and  $\Delta\Delta\text{CT}$  values and power calculations were completed on duplicate averages. Following this, duplicate averages for the four replicates of each microRNA mimic and siRNA transfected/experiment were averaged for a mean power value for each microRNA and siRNA, which was presented on a bar graph. The standard error mean (SEM) for each microRNA and siRNA was calculated using average duplicate  $\Delta\text{CT}$  values and the significance of results was assessed using the two-tailed student's t-test on these values, to a value of  $p < 0.01$ ,  $p < 0.05$  or non-significant.

When averaging qRT-PCR data from all experiments, the mean power values for each microRNA and siRNA from individual experiments were averaged and presented on a bar graph with the SEM and two-tailed student's t-test calculated using the average  $\Delta\text{CT}$  values for each microRNA from each individual experiment. As before, significance was assessed to a value of  $p < 0.01$ ,  $p < 0.05$  or non-significant.

### 2.4. Protein Analysis

#### 2.4.1. Protein Harvest

72 hours after transfection, medium was aspirated from 6-well plates and cells were washed with PBS. PBS was aspirated and cells were lysed with 150 $\mu\text{l}$  RIPA buffer (1.22g Trizma base, 1.8g NaCl, 160ml dH<sub>2</sub>O – pH7.4, 2ml Igepal, 5ml sodium deoxycholate, 2ml 100mM EDTA and protease inhibitor cocktail (6:100 dilution (Sigma)))/well for 20 minutes at -20°C. Lysates were transferred into Eppendorfs, sonicated at 4°C for 1 minute on a medium setting using the Bioruptor Standard (Diagenode), centrifuged at 4°C at 13,000xg for 5 minutes and

lysates were collected. Protein concentrations were determined using the BCA protein assay (ThermoScientific).

#### 2.4.2. Western Blotting

<b>Antibody</b>	<b>Company</b>	<b>Dilution</b>
Rabbit anti-PBF	In house	1:500 (In 5% non-fat milk)
Goat anti-rabbit	Dako	1:2,000 (In 5% non-fat milk)
Mouse anti- $\beta$ -actin	Sigma	1:10,000 (In 5% non-fat milk)
Rabbit anti-mouse	Dako	1:10,000 (In 5% non-fat milk)

**Table 1: Antibodies**

All antibodies used within this investigation listed at the dilution used and the company antibodies were purchased from.

30 $\mu$ g of each protein lysate in protein sample buffer (0.107g DTT (Sigma)/1ml Laemmli buffer (BioRad)) was incubated at 95°C for 5 minutes before being resolved on a 12% SDS-polyacrylamide gel. Proteins were transferred onto a PVDF membrane (GE Life Sciences) and probed with a rabbit anti-PBF primary antibody in 5% non-fat milk at room temperature for 1 hour, washed in TBST (50ml 1M Tris pH7.6, 20g 5mM NaCl, 0.625ml Tween-80 and 2449.4ml dH<sub>2</sub>O) then probed with goat anti-rabbit antibody in 5% non-fat milk at room temperature for 1 hour. Membranes were incubated with Pierce® ECL2 Western blotting substrate (ThermoScientific), placed into a light-excluding cassette and exposed to x-ray film, which was developed by the Xograph Compact X4 film processor.

Following washing in TBST, membranes were re-probed using murine anti  $\beta$ -actin antibody in 5% non-fat milk at room temperature for 1 hour, washed in TBST then probed with rabbit anti-murine antibody in 5% non-fat milk at room temperature for 45 minutes. Membranes

were incubated with Amersham ECL plus Western blotting substrate (GE Life Sciences) and developed as described above.

#### *2.4.3. Statistics*

Densitometry was completed on ImageJ to analyse Western blots, with PBF protein levels at 25kDa and 30kDa (as these are the main forms of PBF studied (Watkins, R.J., et al., 2010) and identified by various antibodies by Western blot) normalised against  $\beta$ -actin. The fold-change relative to the negative control, assigned an arbitrary value of 1.0, was calculated for each microRNA or siRNA and presented on a bar graph. When averaging Western blots from all experiments, the fold-changes relative to the negative control for each microRNA or siRNA from individual experiments were averaged and presented on a bar graph, with the SEM and two-tailed student's t-test completed using the fold-change values. Statistical significance was assessed to a value of  $p < 0.01$ ,  $p < 0.05$  or non-significant.

### 3. RESULTS

#### 3.1. MicroRNAs Predicted to Target PBF

Five microRNAs predicted to target PBF were selected in this investigation, with the evidence and reasons for their selection based on prediction software and the literature, as shown below.

##### 3.1.1. *hsa-miR-1*

MiRWalk identified *hsa-miR-1* to be involved in a validated interaction with PBF (PTTG1P) (Dweep, H., et al., 2011) (Figure 4A). Additionally, it has been described that *miR-1* acts as a tumour suppressor in thyroid tumours due to a downregulation of *miR-1* apparent in thyroid carcinomas compared to normal thyroid tissue (Leone, V., et al., 2011), highlighting this as a particularly interesting microRNA to investigate.

	Gene Name	EntrezID	MicroRNA Name	StemLoopName
A	<a href="#">PTTG1P</a>	754	<a href="#">hsa-miR-1</a>	hsa-mir-1-2
	<a href="#">PTTG1P</a>	754	<a href="#">hsa-miR-1</a>	hsa-mir-1-1
B	<a href="#">PTTG1P</a>	754	<a href="#">hsa-miR-124</a>	hsa-mir-124-1
	<a href="#">PTTG1P</a>	754	<a href="#">hsa-miR-124</a>	hsa-mir-124-2
	<a href="#">PTTG1P</a>	754	<a href="#">hsa-miR-124</a>	hsa-mir-124-3
	<a href="#">PTTG1P</a>	754	<a href="#">hsa-miR-373</a>	hsa-mir-373
	<a href="#">PTTG1P</a>	754	<a href="#">hsa-miR-373*</a>	hsa-mir-373

**Figure 4: Identification of PBF as a validated target of microRNA from miRWalk**

**A)** PTTG1P/PBF is a validated target of *hsa-miR-1* (Dweep, H., et al., 2011).

**B)** PTTG1P/PBF is a validated target of *hsa-miR-124* (Dweep, H., et al., 2011).

##### 3.1.2. *hsa-miR-122-5p*

*hsa-miR-122-5p* was not identified by the prediction software to target PBF however, as described previously, PBF has been shown to be regulated in CHB and HCC by *miR-122*. In addition, inhibition of *miR-122* is described to cause an upregulation of PBF in HCC resulting in a promotion of tumour growth and invasion (Li, C. et al., 2012) making this a particularly interesting microRNA to investigate due to PBF being known to have functions in



proliferation and invasion. In addition, miR-122 has been observed to be downregulated in breast cancer and upon overexpression *in vitro* and *in vivo* inhibits breast cancer cell proliferation (Wang, B., et al., 2012), in line with the previous observations of PBF.

### 3.1.3. *hsa-miR-124-3p*

MiRWalk identified miR-124 to have a validated interaction with PBF (PTTG1IP) (Dweep, H., et al., 2011) (Figure 4B), with additional evidence from miRTarBase, in the form of a microarray, highlighting the same (Hsu, S.D., et al., 2010). Furthermore, TargetScan identified the miR-124 binding site on PBF to be conserved as well as miR-124 itself defined as broadly conserved among vertebrates (Friedman, R.C., et al., 2009) (Figure 5A), which is suggestive of an important role in regulating the genome and more specifically, PBF. In the literature, miR-124 has been described to have a role as a tumour suppressor in various cancers by modulating the proliferation and aggressiveness of tumours (Xu X., et al., 2013).

	miRNA	conserved sites				poorly conserved sites			
		Total	8mer	7mer-m8	7mer-1A	Total	8mer	7mer-m8	7mer-1A
<b>A</b>	miR-124/124ab/506	1	1	0	0	0	0	0	0
	miR-451	0	0	0	0	1	0	1	0
	miR-217	0	0	0	0	1	1	0	0
	miR-196abc	0	0	0	0	1	0	1	0
<b>B</b>	miR-193/193b/193a-3p	0	0	0	0	1	0	1	0
	miR-33a-3p/365/365-3p	1	0	1	0	0	0	0	0
	miR-143/1721/4770	0	0	0	0	1	0	1	0

**Figure 5: Broadly conserved microRNA among vertebrates predicted by TargetScan to target PBF**

**A)** miR-124 and miR-506 are ranked to be broadly conserved microRNAs in vertebrates predicted to target PBF (Friedman, R.C., et al., 2009).

**B)** miR-193b is also ranked to be a broadly conserved microRNA in vertebrates predicted to target PBF (Friedman, R.C., et al., 2009).

### 3.1.4. *hsa-miR-193b-5p*

The miR-193 family, including miR-193b, was predicted by TargetScan to bind to PBF at a poorly conserved site (Friedman, R.C., et al., 2009) (Figure 5B). However, despite having a

poorly conserved binding site on PBF, the miR-193 family is conserved among mammals (Friedman, R.C., et al., 2009) suggestive of an important functional role. The literature described miR-193b to target oestrogen receptor  $\alpha$  (ER- $\alpha$ ), resulting in an inhibition of oestrogen-induced growth of breast tissue tumours (Leivonen, S-K., et al., 2011) (Yoshimoto, N., et al., 2011), which may be pertinent given that PBF is upregulated in ER- $\alpha$  positive MCF7 cells (Watkins, R.J., et al., 2010).

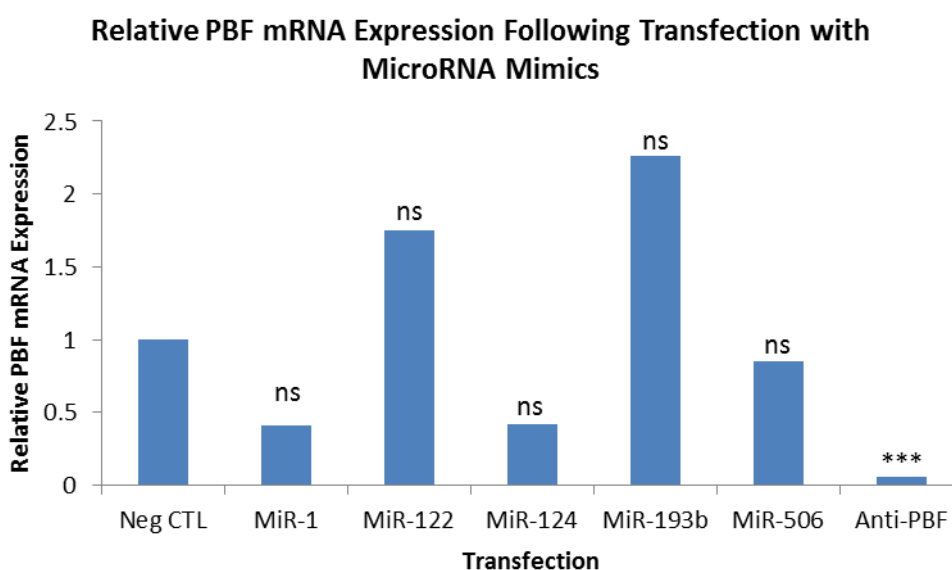
### *3.1.5. hsa-miR-506-3p*

hsa-miR-506 has sequence similarity with hsa-miR-124, resulting in both these microRNAs predicted to bind to the same conserved site on the 3' UTR of PBF as well as both being broadly conserved among vertebrates (Friedman, R.C., et al., 2009) (Figure 5A). Furthermore, hsa-miR-506 has been implicated in suppressing epithelial-mesenchymal transition (EMT) in breast cancer cell lines (Arora, H., et al., 2013) highlighting an importance in cell invasion and migration, which correlates with the observations of PBF playing a role in invasion (Watkins, R.J., et al., 2010).

### 3.2. Effect on PBF mRNA Expression Following MicroRNA Mimic Transfections

#### 3.2.1. Effect on PBF mRNA Expression Following MicroRNA Mimic Transfections in SW1736 Cells

Following the first experiment in SW1736 cells a 94.50% decrease ( $p > 0.01$ ) in PBF mRNA expression was observed as a result of anti-PBF siRNA transfection (Figure 6). Despite this, no significant changes in PBF mRNA expression were observed following any of the microRNA mimic transfections (Figure 6). However, due to technical issues with the RNA isolation and thus RNA quality in this experiment, these results were not thought to be reliable and were not been included in any further analysis.

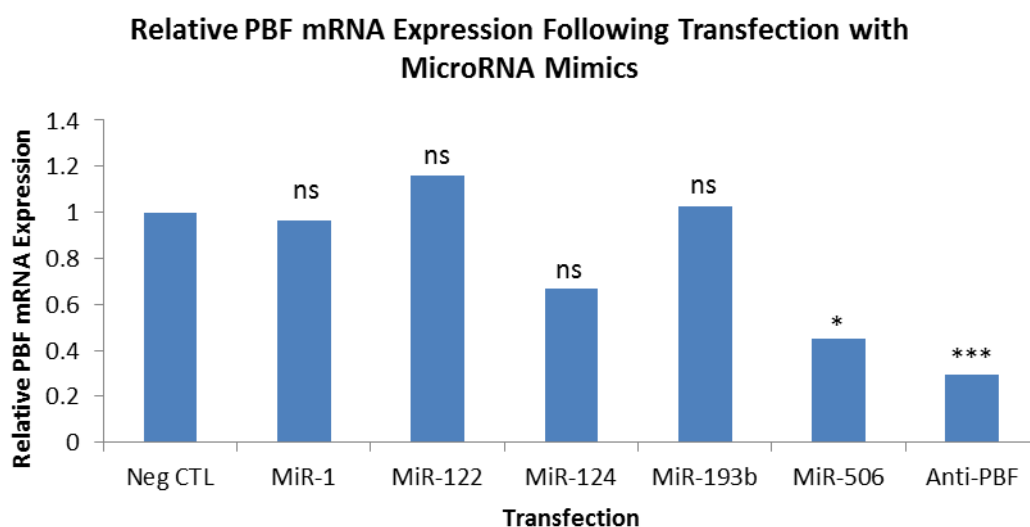


	Neg CTL	MiR-1	MiR-122	MiR-124	MiR-193b	MiR-506	Anti-PBF
$\Delta$ CT	11.58	12.95	10.80	13.09	10.45	11.84	15.88
SEM	0.42	0.46	0.30	0.45	0.27	0.14	0.32

**Figure 6: PBF mRNA Expression in SW1736 cells following transfection with five microRNAs**

PBF mRNA expression in SW1736 cells following the first experiment with (L-R): Negative control (Neg CTL), hsa-miR-1 (MiR-1), hsa-miR-122-5p (MiR-122), hsa-miR-124-3p (MiR-124), hsa-miR-193b-5p (MiR-193b), hsa-miR-506-3p (MiR-506) and anti-PBF siRNA (Anti-PBF) normalised to 18S.  $\Delta$ CT indicates PBF CT value – 18S CT value and SEM indicates the SEM of the four replicates for each sample. Statistics were calculated using the paired t-test, where \*\*\*= $p < 0.01$  and ns=non-significant.

The second experiment in SW1736 cells indicated a significant decrease in PBF mRNA expression following transfection with anti-PBF siRNA of 70.77% ( $p < 0.01$ ) as well as a significant decrease following the transfection with hsa-miR-506-3p of 55.00% ( $p < 0.05$ ). In addition, albeit non-significant, a decrease in PBF mRNA expression was observed following hsa-miR-1 and hsa-miR-124-3p transfection of 3.72% and 33.20% respectively (Figure 7).



	Neg CTL	MiR-1	MiR-122	MiR-124	MiR-193b	MiR-506	Anti-PBF
$\Delta$ CT	10.22	10.64	10.51	11.22	10.05	11.26	11.87
SEM	0.31	0.28	0.46	0.38	0.08	0.15	0.10

**Figure 7: PBF mRNA Expression in SW1736 cells following transfection with five microRNAs**

PBF mRNA expression in SW1736 cells following the second experiment with (L-R): Negative control (Neg CTL), hsa-miR-1 (MiR-1), hsa-miR-122-5p (MiR-122), hsa-miR-124-3p (MiR-124), hsa-miR-193b-5p (MiR-193b), hsa-miR-506-3p (MiR-506) and anti-PBF siRNA (Anti-PBF) normalised to 18S.  $\Delta$ CT indicates PBF CT value – 18S CT value and SEM indicates the SEM of the four replicates for each sample. Statistics were calculated using the paired t-test, where \*\*\*= $p < 0.01$ , \*= $p > 0.05$  and ns=non-significant.

In the third experiment in SW1736 cells, hsa-miR-193b-5p was not investigated as the transfection reagent was limited meaning the microRNA mimic with the least success thus far was sacrificed. The other microRNA mimics were transfected as before, with very small changes in PBF mRNA expression following transfection observed (Figure 8). However,

following anti-PBF siRNA transfection a decrease in mRNA expression of 72.72% ( $p < 0.05$ ) was observed (Figure 8).

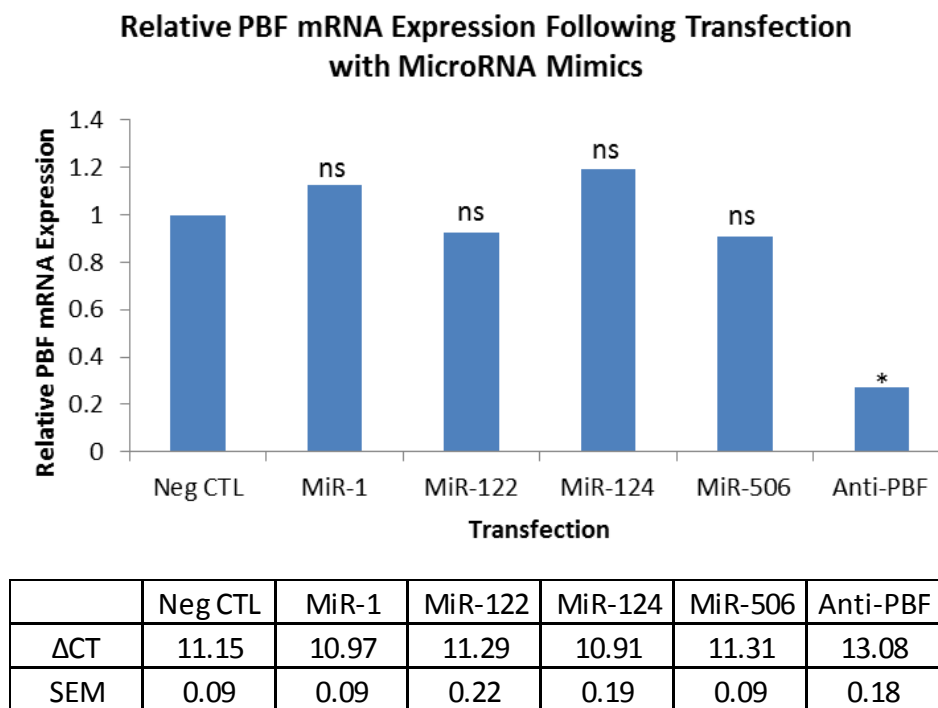
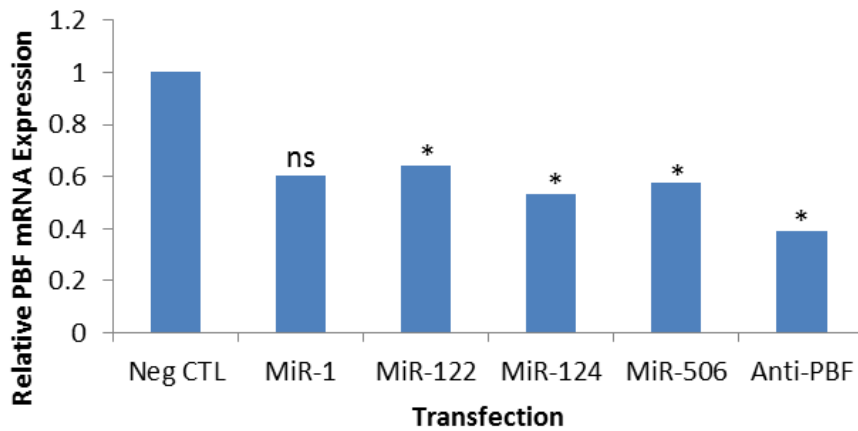


**Figure 8: PBF mRNA Expression in SW1736 cells following transfection with four microRNAs**

PBF mRNA expression in SW1736 cells following the third experiment with (L-R): Negative control (Neg CTL), hsa-miR-1 (MiR-1), hsa-miR-122-5p (MiR-122), hsa-miR-124-3p (MiR-124), hsa-miR-506-3p (MiR-506) and anti-PBF siRNA (Anti-PBF) normalised to 18S.  $\Delta$ CT indicates PBF CT value – 18S CT value and SEM indicates the SEM of the four replicates for each sample. Statistics were calculated using the paired t-test, where  $*$ = $p < 0.05$  and ns=non-significant.

Following the fourth experiment in SW1736 cells, where hsa-miR-193b-5p was also not investigated, anti-PBF siRNA caused a decrease in PBF mRNA expression of 61.00% ( $p < 0.05$ ). In addition, hsa-miR-122-5p, hsa-miR-124-3p and hsa-miR-506-3p caused significant decreases in PBF mRNA expression of 35.80% ( $p < 0.05$ ), 46.97% ( $p < 0.05$ ) and 42.45% ( $p < 0.05$ ) respectively (Figure 9). In addition, hsa-miR-1 also caused a decrease in PBF mRNA expression of 39.43% (non-significant) (Figure 9), however this was non-significant.

### Relative PBF mRNA Expression Following Transfection with MicroRNA Mimics

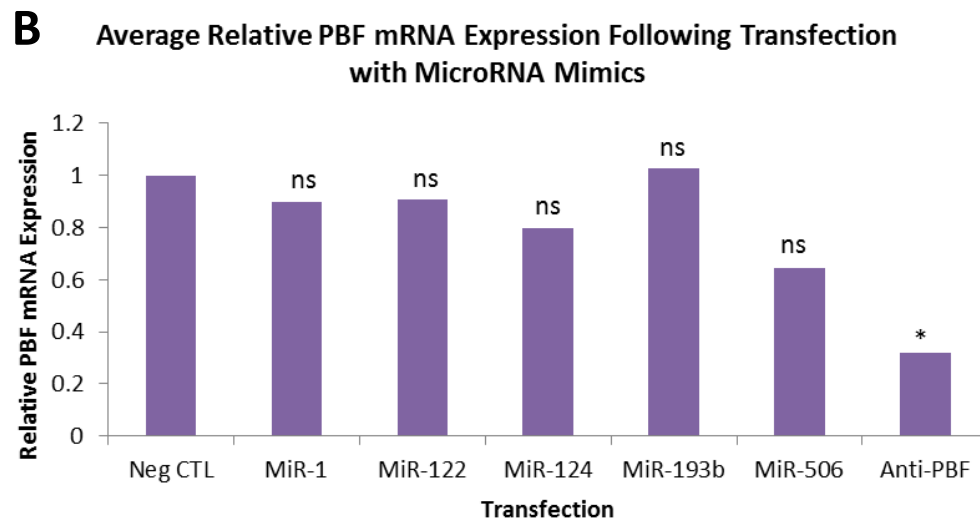
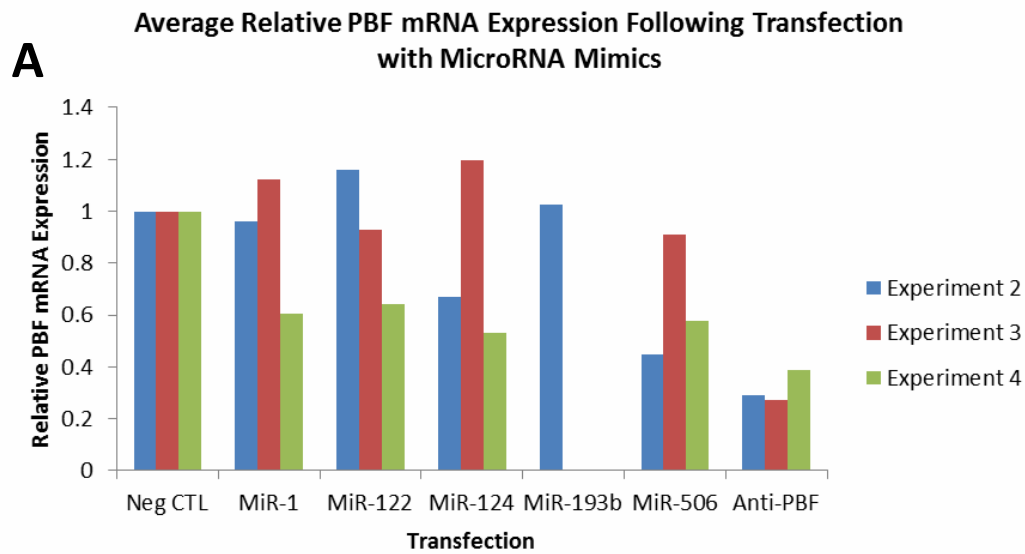


	Neg CTL	MiR-1	MiR-122	MiR-124	MiR-506	Anti-PBF
$\Delta$ CT	10.10	10.93	10.73	11.08	10.95	11.80
SEM	0.17	0.37	0.17	0.32	0.11	0.58

**Figure 9: PBF mRNA Expression in SW1736 cells following transfection with four microRNAs**

PBF mRNA expression in SW1736 cells following the fourth experiment with (L-R): Negative control (Neg CTL), hsa-miR-1 (MiR-1), hsa-miR-122-5p (MiR-122), hsa-miR-124-3p (MiR-124), hsa-miR-506-3p (MiR-506) and anti-PBF siRNA (Anti-PBF) normalised to 18S.  $\Delta$ CT indicates PBF CT value – 18S CT value and SEM indicates the SEM of the four replicates for each sample. Statistics were calculated using the paired t-test, where  $*=p<0.05$  and ns=non-significant.

Average PBF mRNA expression levels were calculated using results from the second, third and fourth experiments, due to technical issues with the RNA from the first experiment. These results can be seen in Figure 10A, with the overall averages and statistics of these in Figure 10B, indicating none of the microRNA mimics caused a significant change in PBF mRNA expression levels overall. The largest decrease in PBF mRNA expression of 35.54% (non-significant) was observed as a result of hsa-miR-506-3p transfection (Figure 10B). However, it is important to note that anti-PBF siRNA caused a significant decrease in PBF mRNA expression levels of 68.16% ( $p<0.05$ ) (Figure 10B), around the value expected from a siRNA.



	Neg CTL	MiR-1	MiR-122	MiR-124	MiR-193b	MiR-506	Anti-PBF
$\Delta$ CT	10.48802	10.84613	10.84204	11.06813	10.054	11.17333	12.24775
SEM	0.330589	0.105105	0.23377	0.089388		0.112329	0.414503

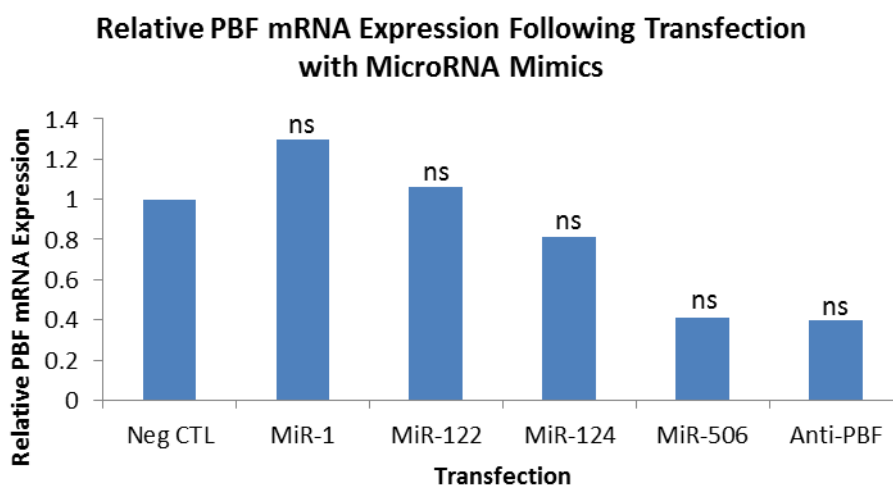
**Figure 10: Average relative PBF mRNA expression following all three transfections in SW1736 cells, with results averaged and analysed**

**A)** Results on relative PBF protein levels following transfection with a negative control (Neg CTL), hsa-miR-1 (MiR-1), hsa-miR-122-5p (MiR-122), hsa-miR-124-3p (MiR-124), hsa-miR-193b-5p, hsa-miR-506-3p (MiR-506) and anti-PBF siRNA (Anti-PBF) (n=3 for all microRNA, except miR-193b-5p (n=1)).

**B)** Average PBF mRNA expression (n=3 for all microRNA, except miR-193b-5p (n=1)), calculated using results in A, with statistics calculated using the paired t-test, where \*=p<0.05 and ns=non-significant.  $\Delta$ CT indicates average  $\Delta$ CT values from three experiments and SEM indicates the SEM from the three experiments. Statistics were calculated using the paired t-test, where \*=p<0.05 and ns=non-significant.

3.2.2. *Effect on PBF mRNA Expression Following MicroRNA Mimic Transfections in MCF7 Cells*

Figure 11 indicates a decrease in PBF mRNA expression of 60.30% (non-significant) following anti-PBF siRNA transfection, as expected. However, none of the transfections with microRNA mimics caused a significant decrease in PBF mRNA expression, with the largest decreases in PBF mRNA expression observed following hsa-miR-124-3p and hsa-miR-506-3p transfections causing decreases in PBF mRNA expression of 18.97% (non-significant) and 59.20% (non-significant) respectively (Figure 11).



	Neg CTL	MiR-1	MiR-122	MiR-124	MiR-506	Anti-PBF
$\Delta$ CT	11.89	12.19	12.43	12.80	12.70	13.04
SEM	0.35	0.29	0.21	0.16	0.30	0.63

**Figure 11: PBF mRNA Expression in MCF7 cells following transfection with four microRNAs**

PBF mRNA expression in MCF7 cells following the first experiment with (L-R): Negative control (Neg CTL), hsa-miR-1 (MiR-1), hsa-miR-122-5p (MiR-122), hsa-miR-124-3p (MiR-124), hsa-miR-506-3p (MiR-506) and anti-PBF siRNA (Anti-PBF) normalised to 18S.  $\Delta$ CT indicates PBF CT value – 18S CT value and SEM indicates the SEM of the four replicates for each sample. Statistics were calculated using the paired t-test, where ns=non-significant.



Following the second experiment in MCF7, despite a non-significant 16.62% decrease in PBF mRNA expression following anti-PBF siRNA transfection, a significant decrease in PBF mRNA expression of 37.75% ( $p < 0.05$ ) was observed following transfection with hsa-miR-124-3p (Figure 12). In comparison, following transfection with the other microRNA mimics; hsa-miR-1, hsa-miR-122-5p and hsa-miR-506-3p all caused an increase in PBF mRNA expression (Figure 12).

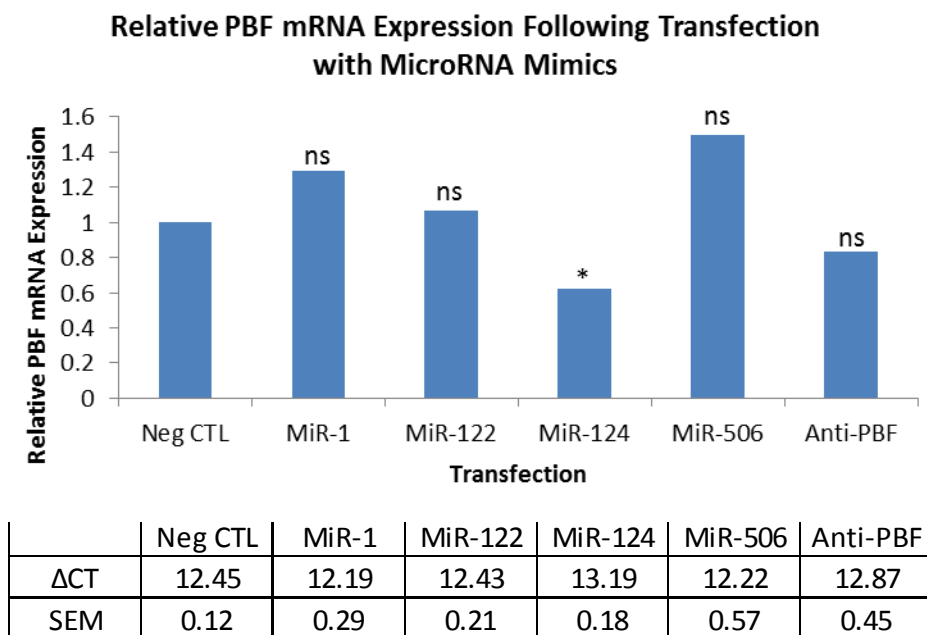


**Figure 12: PBF mRNA Expression in MCF7 cells following transfection with four microRNAs**

PBF mRNA expression in MCF7 cells following the second experiment with (L-R): Negative control (Neg CTL), hsa-miR-1 (MiR-1), hsa-miR-122-5p (MiR-122), hsa-miR-124-3p (MiR-124), hsa-miR-506-3p (MiR-506) and anti-PBF siRNA (Anti-PBF) normalised to 18S.  $\Delta$ CT indicates PBF CT value – 18S CT value and SEM indicates the SEM of the four replicates for each sample. Statistics were calculated using the paired t-test, where  $*$ = $p > 0.05$  and ns=non-significant.

Overall average results for the effect of microRNA mimic transfections on PBF mRNA expression in MCF7 cells were not completed as there were only two sets of data and thus a meaningful average could not be obtained. However, hsa-miR-124-3p was only the microRNA that decreased PBF mRNA expression in both experiments in MCF7 cells.

### **3.3. Effect on PBF Protein Levels Following MicroRNA Mimic Transfections**

It is important to note there are multiple forms of PBF protein, which are recognised by the PBF antibody used during Western blotting - due to PBF having phosphorylation sites, five glycosylation sites as well as the ability to oligomerise (Smith V. and McCabe, C., 2008). However, the two species that were studied in this investigation were at 25kDa and 30kDa, as these are the main forms normally studied (Watkins, R.J., et al., 2010) and identified by Western blot by other commercially available antibodies.

#### *3.3.1. Effect on PBF Protein Levels Following MicroRNA Mimic Transfections in SW1736 Cells*

Figure 13A shows the Western blot following the first experiment in SW1736 cells, highlighting the 25kDa and 30kDa PBF protein bands alongside  $\beta$ -actin. The largest overall effect on PBF protein levels was observed following hsa-miR-122-5p and hsa-miR-124-3p transfection (Figure 13A). Densitometry indicated that at 25kDa and 30kDa, hsa-miR-122-5p caused decreases in PBF protein of 58.30% at 25kDa and 79.66% at 30kDa and hsa-miR-124-3p caused a decrease of 65.70% and 78.11% at 30kDa (Figure 13B). Furthermore, hsa-miR-506-3p also caused large decreases in PBF protein levels at 25kDa and 30kDa of 89.97% and 45.93% respectively (Figure 13B). In addition, following the anti-PBF siRNA transfection a decrease in PBF protein levels of 65.77% at 25kDa and 66.47% at 30kDa (Figure 13B) was observed, as would be expected.

**Figure 13: PBF protein levels in SW1736 cells following transfection with five microRNAs**

**A)** Western blot showing PBF protein levels (\*=25kDa, \*=30kDa) in SW1736 cells following the first experiment with (L-R): Negative control (Neg CTL), hsa-miR-1 (MiR-1), hsa-miR-122-5p (MiR-122), hsa-miR-124-3p (MiR-124), hsa-miR-193b-5p (MiR-193b), hsa-miR-506-3p (MiR-506) and anti-PBF siRNA (Anti-PBF). Anti-β-actin at 44kDa shows approximately equal loading.

**B)** Densitometry of Western blot normalised to β-actin showing PBF protein levels at 25kDa and 30kDa in SW1736 cells relative to the negative control, assigned an arbitrary value of 1.

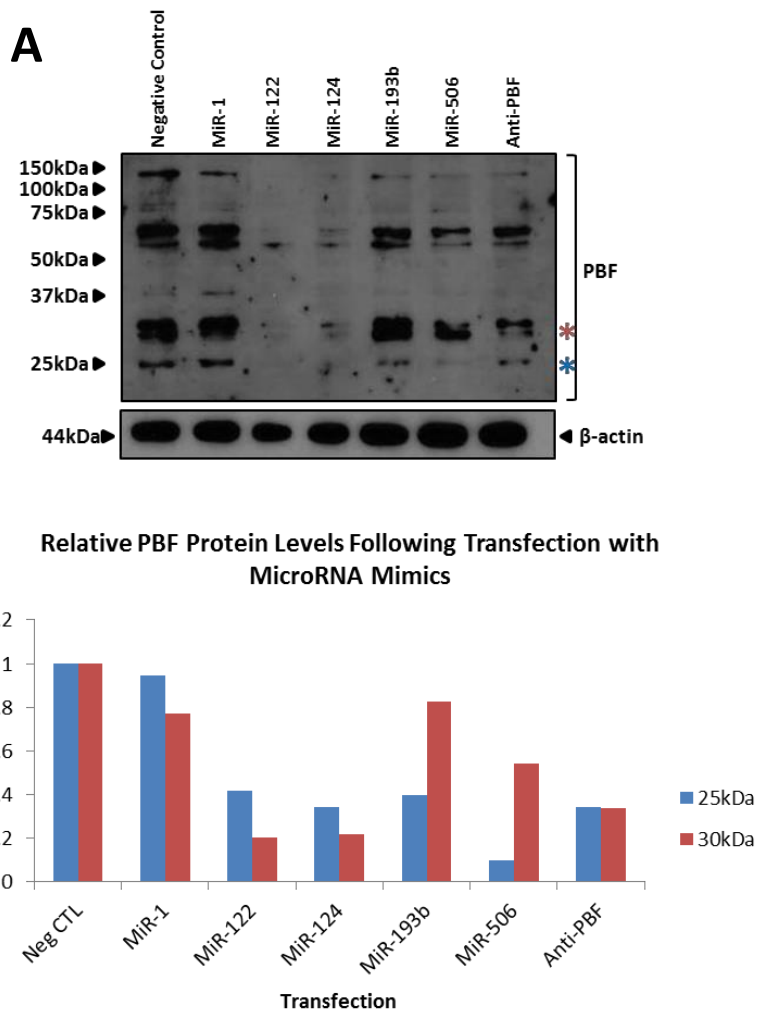


Figure 14A shows the 25kDa and 30kDa PBF protein bands on the Western blot alongside  $\beta$ -actin following the second experiment in SW1736 cells. Figure 14B displays the densitometry from this Western blot indicating a decrease in PBF protein levels following transfection with hsa-miR-1 of 28.42% at 25kDa and 67.27% at 30kDa and hsa-miR-122-5p of 16.34% at 25kDa and 2.31% at 30kDa (Figure 14B). However, hsa-miR-124-3p, hsa-miR-193b-5p and hsa-miR-506-3p all caused an increase in PBF protein levels at 25kDa and 30kDa. Furthermore, unexpectedly, anti-PBF siRNA resulted in an increase in PBF protein levels of 126.01% at 25kDa and 136.08% at 30kDa (Figure 14B) creating some doubt as to how reliable these results are as a decrease following anti-PBF siRNA transfection would be expected as observed for mRNA expression levels following anti-PBF transfection, which was completed at the same time (Figure 10).

**Figure 14: PBF protein levels in SW1736 cells following transfection with five microRNAs**

**A)** Western blot showing PBF protein levels (\*=25kDa, \*=30kDa) in SW1736 cells following the second experiment with (L-R): Negative control (Neg CTL), hsa-miR-1 (MiR-1), hsa-miR-122-5p (MiR-122), hsa-miR-124-3p (MiR-124), hsa-miR-193b-5p (MiR-193b), hsa-miR-506-3p (MiR-506) and anti-PBF siRNA (Anti-PBF). Anti- $\beta$ -actin at 44kDa shows approximately equal loading.

**B)** Densitometry of Western blot normalised to  $\beta$ -actin showing PBF protein levels at 25kDa and 30kDa in SW1736 cells relative to the negative control, assigned an arbitrary value of 1.

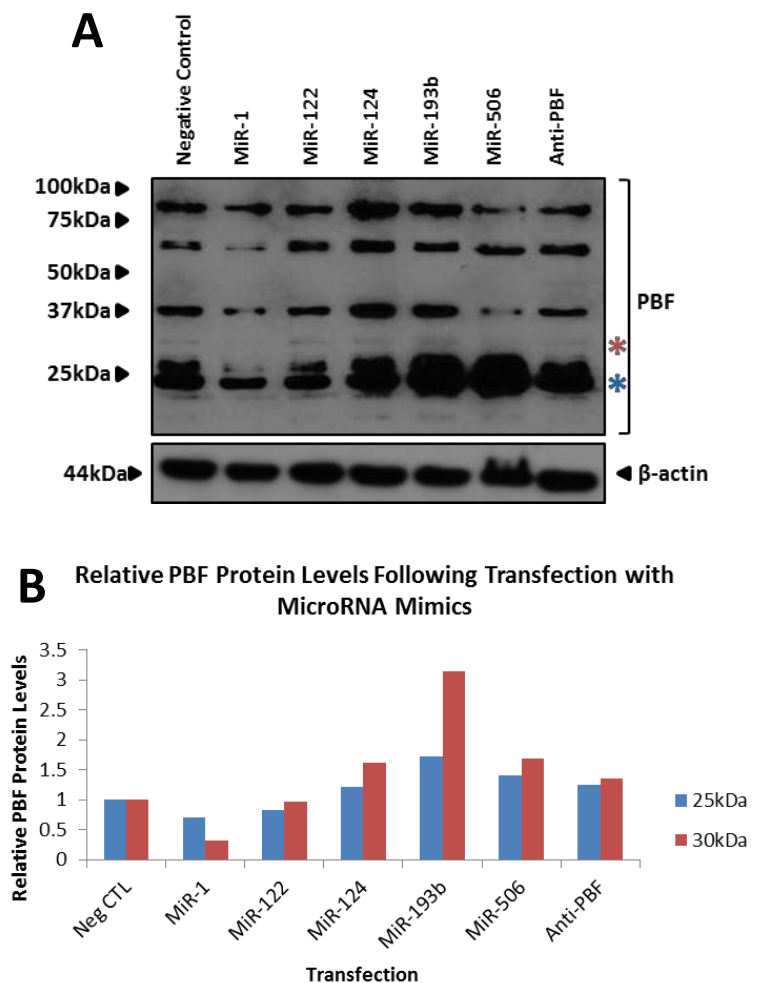
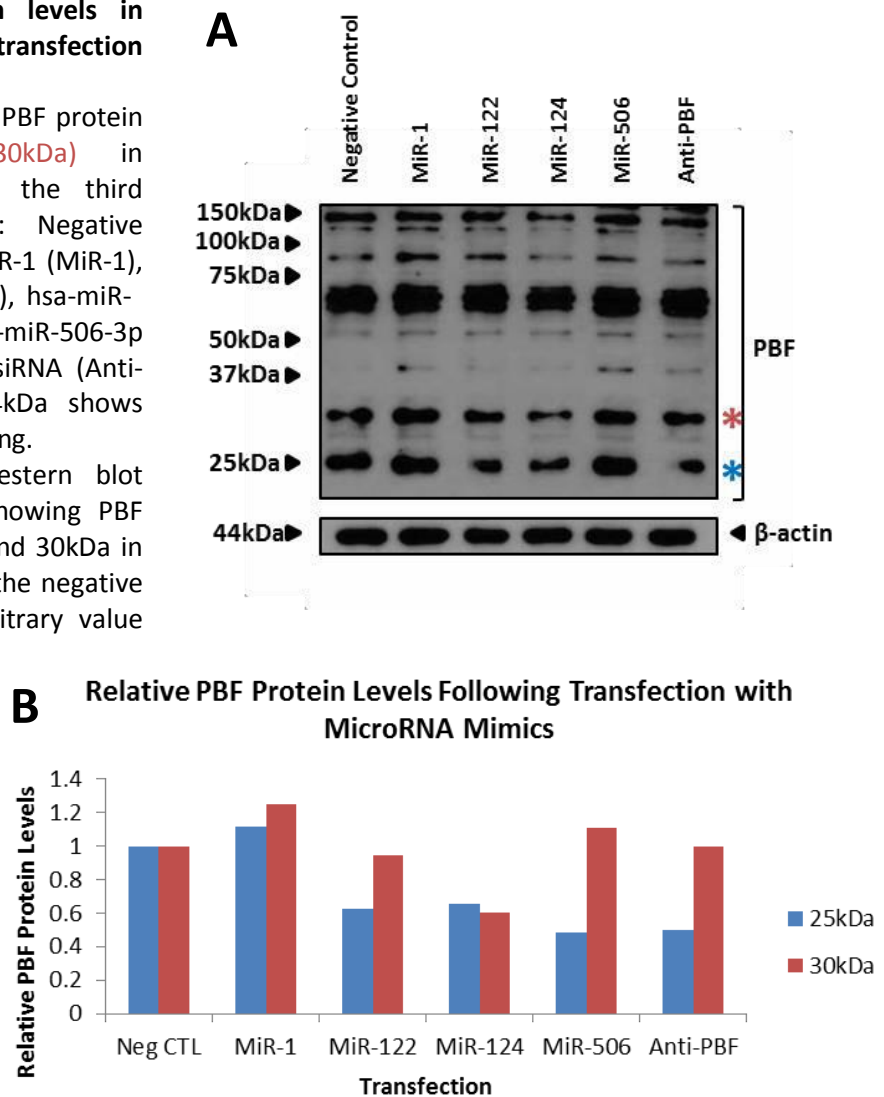


Figure 15A shows the Western blot following the first experiment in SW1736 cells, highlighting the 25kDa and 30kDa PBF protein bands alongside  $\beta$ -actin. It is important to note that hsa-miR-193b-5p was not investigated in this experiment, as transfection reagent was limited - as described previously. Densitometry indicates decreased PBF protein levels following transfection with hsa-miR-122-5p of 37.27% at 25kDa and 5.65% at 30kDa and with hsa-miR-124-3p of 34.35% at 25kDa and 39.92% at 30kDa respectively (Figure 15B). In addition, following anti-PBF siRNA transfection a 49.85% decrease at 25kDa and a 0.24% decrease at 30kDa in PBF protein levels was observed (Figure 15B).

**Figure 15: PBF protein levels in SW1736 cells following transfection with four microRNAs**

**A)** Western blot showing PBF protein levels (\*=25kDa, \*=30kDa) in SW1736 cells following the third experiment with (L-R): Negative control (Neg CTL), hsa-miR-1 (MiR-1), hsa-miR-122-5p (MiR-122), hsa-miR-124-3p (MiR-124), hsa-miR-506-3p (MiR-506) and anti-PBF siRNA (Anti-PBF). Anti- $\beta$ -actin at 44kDa shows approximately equal loading.

**B)** Densitometry of Western blot normalised to  $\beta$ -actin showing PBF protein levels at 25kDa and 30kDa in SW1736 cells relative to the negative control, assigned an arbitrary value of 1.

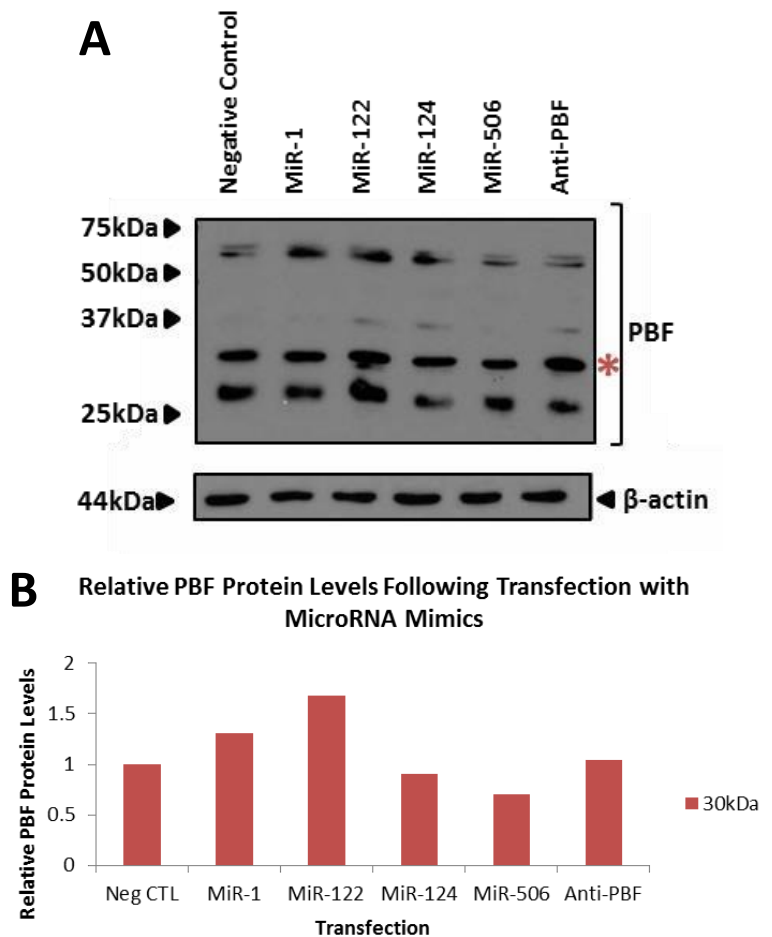


Following the fourth experiment in SW1736 cells, the 25kDa PBF protein band, which was previously identified and quantified, was not visible by Western blot. Therefore, only the 30kDa PBF protein band (Figure 16A) was quantified by densitometry (Figure 16B). Results indicated the anti-PBF siRNA transfection caused an increase in PBF protein levels of 104.51% (Figure 16B), similar to the previous unexpected observation (Figure 14B). However, despite this, a decrease in PBF protein levels at 30kDa was observed following transfection with hsa-miR-124 and hsa-miR-506-3p of 9.55% and 29.46% respectively (Figure 16B).

**Figure 16: PBF protein levels in SW1736 cells following transfection with four microRNAs**

**A)** Western blot showing PBF protein levels (\*=30kDa) in SW1736 cells following the fourth experiment with (L-R): Negative control (Neg CTL), hsa-miR-1 (MiR-1), hsa-miR-122-5p (MiR-122), hsa-miR-124-3p (MiR-124), hsa-miR-506-3p (MiR-506) and anti-PBF siRNA (Anti-PBF). Anti-β-actin at 44kDa shows approximately equal loading.

**B)** Densitometry of Western blot normalised to β-actin showing PBF protein levels at 30kDa in SW1736 cells relative to the negative control, assigned an arbitrary value of 1.



The results from the four experiments above on PBF protein levels at 25kDa in SW1736 cells are shown together in Figure 17A; indicating experiment two as a potential anomaly.

However, due to small n numbers making it difficult to determine a true anomaly, results were averaged from all sets of data and statistics completed (Figure 17B), indicating a significant average decrease in PBF protein levels following transfection with hsa-miR-122-5p of  $37.32 \pm 12.10$  ( $p > 0.05$ ) (Figure 17B). In addition, hsa-miR-124-3p and hsa-miR-506-3p caused an average decrease of  $26.21 \pm 25.48\%$  (non-significant) and  $33.66 \pm 38.85\%$  (non-significant) (Figure 17B), albeit non-significant. The average decrease in PBF protein levels at 25kDa following transfection with anti-PBF siRNA was  $29.87 \pm 28.32\%$  (non-significant) (Figure 17B), lower than expected.

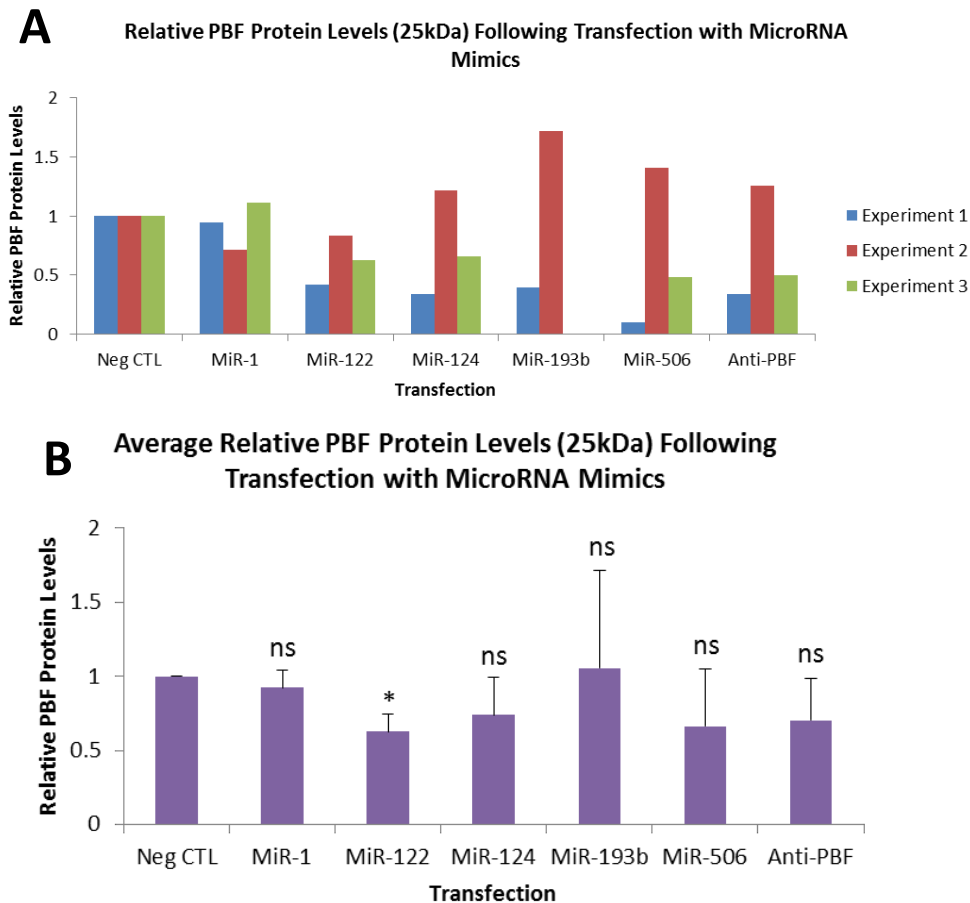


**Figure 17: Average relative PBF protein levels (25kDa) following all three experiments in SW1736 cells, with results averaged and analysed**

**A)** Results on relative PBF protein levels following transfection with a negative control (Neg CTL), hsa-miR-1 (MiR-1), hsa-miR-122-5p (MiR-122), hsa-miR-124-3p (MiR-124), hsa-miR-193b-5p, hsa-miR-506-3p (MiR-506) and anti-PBF siRNA (Anti-PBF) ( $n=3$  for all microRNA, besides miR-193b-5p ( $n=2$ )).

**B)** Average PBF protein levels ( $n=3$  for all microRNA, besides miR-193b-5p ( $n=2$ )), calculated using results in A, with statistics calculated using the paired t-test, where  $*=p < 0.05$  and ns=non-significant and error bars are calculated from the SEM.

The results from the four experiments above on PBF protein levels at 30kDa in SW1736 cells are shown in Figure 18A, highlighting experiment two as a potential anomaly, similarly to what was shown in Figure 17A. However, results were averaged from all sets of data and statistics completed (Figure 18B), which indicated none of the microRNA mimics or anti-PBF siRNA caused a significant average decrease in PBF protein levels at 30kDa. The largest average decrease in PBF protein levels was due to hsa-miR-124-3p, which caused a decrease of  $16.35 \pm 29.70\%$  (non-significant) at 30kDa (Figure 18B).

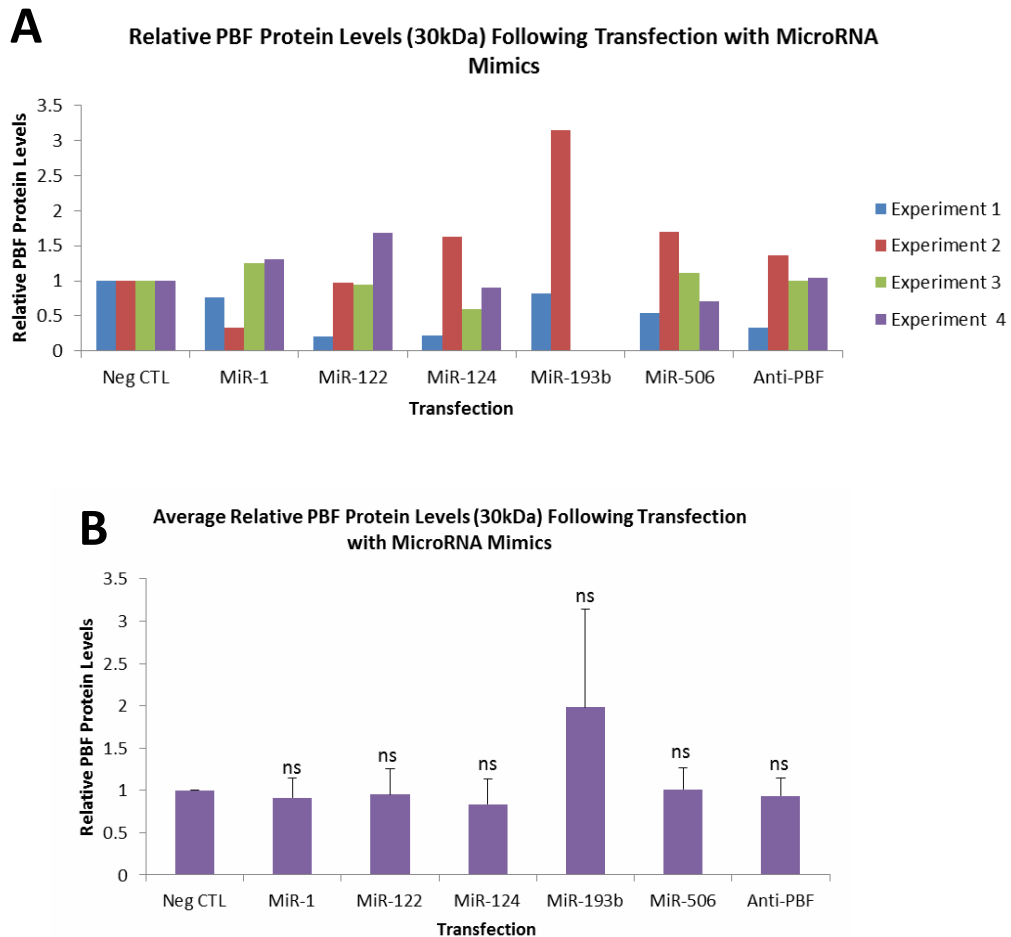


**Figure 18: Average relative PBF protein levels (30kDa) following all four experiments in SW1736 cells, with results averaged and analysed**

**A)** Results on relative PBF protein levels following transfection with a negative control (Neg CTL), hsa-miR-1 (MiR-1), hsa-miR-122-5p (MiR-122), hsa-miR-124-3p (MiR-124), hsa-miR-193b-5p, hsa-miR-506-3p (MiR-506) and anti-PBF siRNA (Anti-PBF) (n=4 for all microRNA, besides miR-193b-5p (n=2)).

**B)** Average PBF protein levels (n=3 for all microRNA, besides miR-193b-5p (n=2)), calculated using results in A, with statistics calculated using the paired t-test, where ns=non-significant and error bars are calculated from the SEM.



When observing the effect of microRNA mimics on PBF protein levels at both 25kDa and 30kDa, it appeared that all the selected microRNA mimics had a greater effect at 25kDa (Figure 19). Overall, hsa-miR-122-5p, hsa-miR-124-3p and hsa-miR-506-3p transfections all caused a similar degree of effect on PBF protein levels at 25kDa and 30kDa, which was comparable to the effect following anti-PBF siRNA transfection (Figure 19) suggestive of a potential of these microRNAs in regulating PBF.

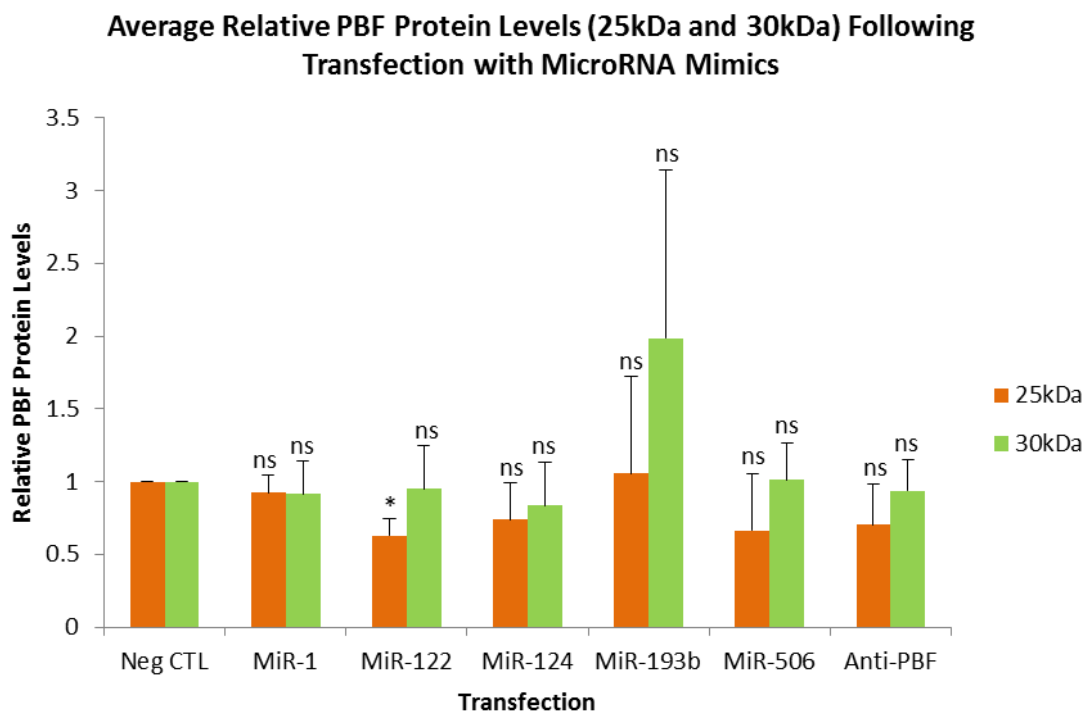


**Figure 19: Comparison of average relative PBF protein levels (25kDa and 30kDa) following experiments in SW1736 cells**

Average PBF protein levels (From Figure 17B and Figure 18B, with statistics calculated using the paired t-test, where  $*=p<0.05$  and ns=non-significant and error bars are calculated from the SEM.

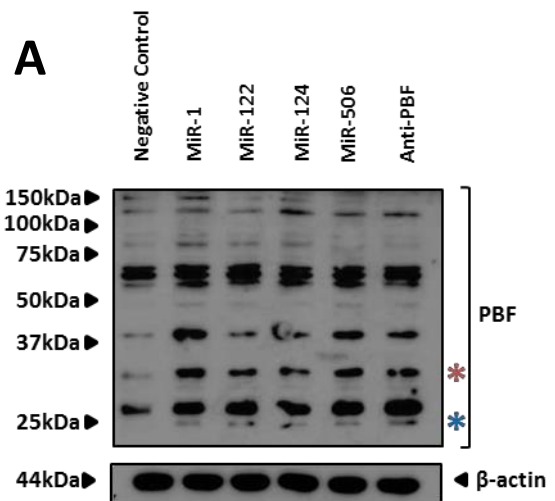
### 3.3.2. Effect on PBF Protein Levels Following MicroRNA Mimic Transfections in MCF7 Cells

The Western blot following the first experiment in MCF7 cells can be seen in Figure 20A, with the 25kDa and 30kDa PBF protein bands highlighted alongside  $\beta$ -actin. Densitometry indicated all transfections caused large increases in PBF protein levels at both 25kDa and 30kDa (Figure 20B), highlighting there may have been a technical issue with these transfections as even the anti-PBF siRNA caused an increase in the surplus of 700%.

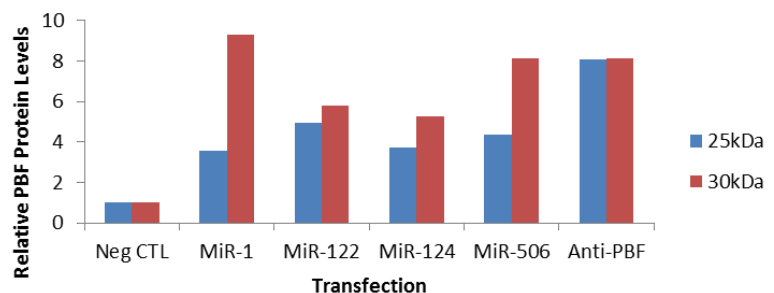
**Figure 20: PBF protein levels in MCF7 cells following transfection with four microRNAs**

**A)** Western blot showing PBF protein levels (\*=25kDa, \*=30kDa) in MCF7 cells following the first experiment with (L-R): Negative control (Neg CTL), hsa-miR-1 (MiR-1), hsa-miR-122-5p (MiR-122), hsa-miR-124-3p (MiR-124), hsa-miR-506-3p (MiR-506) and anti-PBF siRNA (Anti-PBF). Anti- $\beta$ -actin at 44kDa shows approximately equal loading.

**B)** Densitometry of Western blot normalised to  $\beta$ -actin showing PBF protein levels at 25kDa and 30kDa in MCF7 cells relative to the negative control, assigned an arbitrary value of 1.



**B) Relative PBF Protein Levels Following Transfection with MicroRNA Mimics**



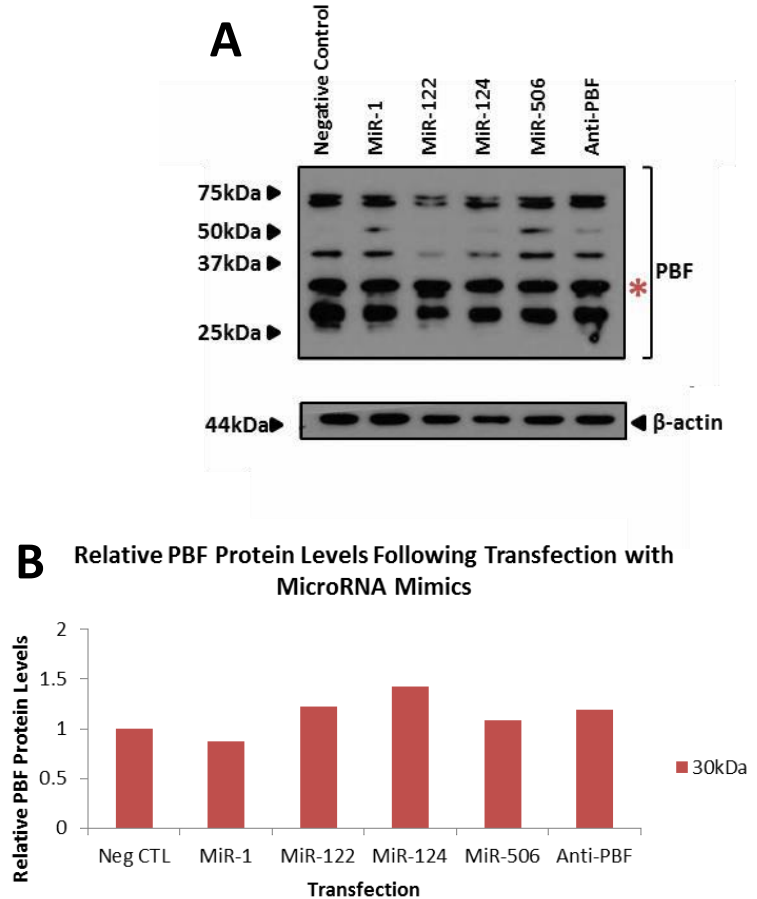
Following the second experiment in MCF7 cells, the Western blot indicated the 30kDa PBF protein band (Figure 21A) but the PBF antibody did not identify the 25kDa PBF protein band, as seen previously in Figure 16A. Despite this, densitometry was completed for the 30kDa

PBF protein band, which indicated only hsa-miR-1 caused a small decrease in PBF protein levels of 12.95% (Figure 21B).

**Figure 21: PBF protein levels in MCF7 cells following transfection with four microRNAs**

**A)** Western blot showing PBF protein levels (\*=30kDa) in MCF7 cells following the second experiment with (L-R): Negative control (Neg CTL), hsa-miR-1 (MiR-1), hsa-miR-122-5p (MiR-122), hsa-miR-124-3p (MiR-124), hsa-miR-506-3p (MiR-506) and anti-PBF siRNA (Anti-PBF). Anti-β-actin at 44kDa shows approximately equal loading.

**B)** Densitometry of Western blot normalised to β-actin showing PBF protein levels at 30kDa in MCF7 cells relative to the negative control, assigned an arbitrary value of 1.



Average results of the effect of microRNA mimic transfections on PBF protein levels in MCF7 cells was not completed due to two reasons: firstly, only one data set was available for the 25kDa PBF protein band and secondly, the 30kDa protein band gave variable results within the two sets of results making it impossible to obtain a true average result.

## 4. DISCUSSION

Due to the observation of PBF being overexpressed in thyroid cancers (Smith, V.E., et al., 2013) and microRNAs being described to be deregulated in thyroid cancers (Vriens, M.R., et al., 2012), it was hypothesised that there may be a correlation between microRNA deregulation and PBF overexpression. Therefore, this investigation was designed to identify microRNAs that target PBF as well as challenging the findings of Li, C., et al., who described PBF as a target of hsa-miR-122 in liver cancer (2013). Consequently, in this investigation, it was identified that hsa-miR-122-5p, hsa-miR-124-3p and hsa-miR-506-3p all targeted PBF to some degree, resulting in decreased PBF mRNA expression and/or protein levels. Subsequently, this may highlight a mechanism for the regulation of PBF, which is currently fairly elusive, whereby microRNA deregulation contributes to the overexpression of PBF, leading to thyroid cancer.

### 4.1. hsa-miR-122-5p Decreased PBF Protein Levels

The most striking average decrease in PBF protein levels following microRNA mimic transfection was observed following transfection with hsa-miR-122-5p in SW1736 cells, which caused a significant decrease in PBF protein levels at 25kDa of  $37.32 \pm 12.10$  ( $p > 0.05$ ), which was greater than the average decrease following anti-PBF siRNA transfection of  $29.87 \pm 28.32\%$  (non-significant) (Figure 17B).

However, a similar effect of hsa-miR-122-5p against PBF was not observed at 30kDa (Figure 18) in SW1736 cells or at 25kDa or 30kDa in MCF7 cells (Figures 20 and 21). Subsequently, further investigations would need to take place in both these cell lines, particularly MCF7 cells to increase the number of repeats before a full conclusion could be made on whether hsa-miR-122-5p targets PBF. In addition, it would be essential to extend the investigation to study

the other forms of PBF protein, including the larger protein bands representing dimers, as in this investigation limitations meant only the main forms of PBF at 25kDa and 30kDa (Watkins, R.J., et al., 2010) were observed.

Furthermore, despite the decrease in PBF protein levels at 25kDa, it is important to note that PBF mRNA expression levels were not significantly altered by hsa-miR-122-5p in this investigation, with an average decrease of only 9.07% (non-significant) observed following transfection in SW1736 cells (Figure 10). This may indicate that PBF is not being directly targeted by hsa-miR-122-5p, but instead is being affected by hsa-miR-122-5p targeting another protein or pathway, which subsequently alters PBF protein levels. This is possible as each microRNA has approximately 200 mRNA targets (Carther, R.W., 2006), meaning even if PBF was directly targeted by hsa-miR-122-5p other mRNAs would also be targeted. To confirm whether PBF is being targeted directly by hsa-miR-122-5p, a green fluorescent protein (GFP) reporter assay could be used, by sub-cloning PBF's WT 3'UTR microRNA target site into a GFP vector it could be observed whether hsa-miR-122-5p caused an inhibition of GFP expression.

If the observation of hsa-miR-122-5p decreasing PBF protein levels was confirmed this would be very interesting, as it complements the observations made by Li, C., et al. who described miR-122 targeted PBF in a Huh7 hepatocellular carcinoma cell line (2012). Furthermore, as Li, C., et al. also observed low miR-122 levels correlated with an upregulation of PBF in HCC (Li, C., et al., 2012) this highlights the importance of investigating hsa-miR-122 and PBF in the context of thyroid cancer. In a future investigation it would be interesting to investigate whether the targeting of PBF by hsa-miR-122-5p in SW1736 cells, an anaplastic thyroid carcinoma cell line, can be translated into cases of ATC in patients. This could be achieved by isolating RNA from ATC patient samples and completing qRT-PCR using

TaqMan assays for PBF and hsa-miR-122-5p, with a negative correlation expected between these in thyroid tumour samples compared to in normal thyroid samples. In addition, it would be interesting to observe there correlation between PBF and hsa-miR-122-5p in MTC, FTC and PTC.

#### **4.2. hsa-miR-124-3p and hsa-miR-506-3p Decreased PBF mRNA Expression and Protein Levels**

The largest average decrease in PBF mRNA expression following transfection with a microRNA mimic was observed following hsa-miR-506-3p transfection in SW1736 cells. hsa-miR-506-3p transfection caused a decrease in PBF mRNA expression relative to the negative control of 35.54% in SW1736 cells (Figure 10), although it is important to note this was non-significant. In addition, the PBF protein levels at 25kDa in SW1736 cells were also decreased, by  $33.66\pm 38.85\%$  (non-significant) (Figure 17B) strengthening the likelihood of hsa-miR-506-3p targeting PBF directly.

As hsa-miR-506-3p shared a sequence similarity with hsa-miR-124-3p, resulting in binding at the same site on the 3' UTR of PBF (Dweep, H., et al., 2011), it was interesting to observe that despite hsa-miR-124-5p not having as great an effect as hsa-miR-506-3p on PBF, it still caused an average decrease in PBF mRNA expression levels of 20.25% in SW1736 cells (non-significant) (Figure 10 and an average decrease in PBF protein levels of  $26.21\pm 25.48\%$  (non-significant) at 25kDa in SW1736 cells (Figure 17B). However, due to there not being enough data within this investigation to observe whether a similar effect takes place in MCF7 cells with hsa-miR-124-3p and hsa-miR-506-3p, as well as data not being significant for SW1736 cells, it would be essential to repeat these studies in both cell lines to identify

whether these microRNAs can negatively regulate PBF at both the mRNA expression and protein level.

If hsa-miR-124-3p and hsa-miR-506-3p were confirmed to cause a decrease in PBF mRNA expression and protein levels this would be an interesting observation as despite the prediction of these microRNAs binding to the 3' UTR of PBF (Dweep, H., et al., 2011) there is currently no previous evidence of these microRNAs altering PBF mRNA expression or protein levels. In addition, as both hsa-miR-124-3p and hsa-miR-506-3p are conserved microRNAs with a conserved binding site on PBF (Friedman, R.C., et al., 2009) (Figure 5A) this is suggestive of a potential important role in regulating the genome and as a result deregulation of these microRNAs may result in PBF overexpression, which may lead to the initiation of thyroid tumourigenesis. Previously, miR-124 has been shown to have a role as a tumour suppressor in bladder cancer by modulating the proliferation and aggressiveness of tumours (Xu X., et al., 2013) and hsa-miR-506 has been defined as a 'master suppressor of EMT in breast cancer' (Arora, H., et al., 2013), which is interesting due to the previous observations of PBF playing roles in both proliferation and invasion (Read, M.L., et al., 2011, Watkins, R.J., et al., 2010).

### **4.3. Limitations**

The first limitation in this investigation was with respect to the initial stage in identifying microRNAs that target PBF. Due to both cost and time restrictions only five microRNAs were selected, which was only a handful of the potential microRNAs predicted to target PBF. Furthermore, due to the prediction software used being known to identify false positives, for example TargetScan has been described to identify false positives at a rate of 22-31% (Bentwich, I., 2005), there was potential for selected microRNAs to not actually target PBF.

Therefore, in the future it would be more useful to transfect a range of thyroid carcinoma cell lines with a large library of microRNA mimics, validate results by microarray and then select a larger group of microRNAs for qRT-PCR and Western blot analysis, as done in this investigation, to confirm whether they alter PBF mRNA expression and protein levels.

Another limitation within this investigation, as a result of time restrictions, was the conditions used within this investigation, which were based upon previous observations in the McCabe lab and were not optimised. Therefore, if this investigation was repeated, it would be essential to optimise the time points for RNA isolation and more importantly protein harvest, as the exact half-life of PBF remains unknown. In addition, as the endogenous concentration of microRNAs was not quantified in either the SW1736 or MCF7 cells this may have resulted in a skew in results due to total microRNA concentration following transfection being different not only between microRNAs but also cell lines. Therefore, in a future investigation, qRT-PCR could be used to determine endogenous expression of selected microRNAs and then the concentrations of microRNA mimics required for transfection could be optimised and then normalised with respect to this, allowing a fair comparison to be made between individual microRNAs in each cell line.

Potentially as a result of conditions not being optimised, there were some surprising inconsistencies observed between PBF mRNA expression and protein levels. For example, following the use of anti-PBF siRNA, which is designed to target PBF, there was an average decrease in PBF mRNA expression of 68.16% ( $p > 0.05$ ) in SW1736 cells (Figure 10) within the range expected from a siRNA. However, no significant decrease in PBF protein levels at either 25kDa or 30kDa were observed in SW1736 cells (Figure 19). This was unexpected as lowered mRNA levels account for >84% of the decreased protein production (Guo, H. et al., 2010), which is not in line with what was observed in this investigation. Beyond optimising



conditions, another factor to consider is the PBF antibody used; as it is potentially unreliable, indicating Western blotting may not have been a good representation of the effect of microRNAs on PBF protein levels. In a future investigation it may be beneficial to either use a commercial antibody for Western blotting, for example PBF Antibody (E-8): sc-376960 (Santa Cruz Biotechnology), which binds to the PBF C-terminus identifying PBF at between 23kDa and 34kDa. Alternatively, another option in the future, which may solve the inconsistencies between mRNA and protein as well as issues with the antibody, would be via use of the novel QuantiGene FlowRNA *in situ* hybridisation assay (Affymetrix). Despite currently having no probe sets available for PBF, this assay has the benefit of being able to compare the kinetics of RNA expression and protein levels within a single cell and has been described to be useful for measuring target expression levels when antibodies are inadequate.

#### **4.4. Future Research**

Once conditions were optimised and if hsa-miR-122-5p, hsa-miR-124-3p and hsa-miR-506-3p were each confirmed to target PBF, it would then be useful to complete functional assays to determine the impact at the cellular level following microRNA mimic transfections of these microRNAs in a range of thyroid carcinoma cell lines. It would be interesting to investigate proliferation and invasion, using a MTT proliferation assay and invasion assay respectively, as not only are these factors characteristic of cancer, but PBF has also been shown to induce both proliferation (Read, M.L., et al., 2011) and invasion (Watkins, R.J., et al., 2010). However, as mentioned previously, due to the range of mRNA targets that each microRNA has it would be important to bear in mind that any functional effects observed may not necessarily be due to the effect of microRNAs on PBF.

Following this, it would then be essential to observe whether there is a correlation between hsa-miR-122-5p, hsa-miR-124-3p or hsa-miR-506-3p and PBF in thyroid cancer patient samples using qRT-PCR, in a method similar to that described in 4.1. If microRNAs were identified to be downregulated in thyroid tumours resulting in a subsequent increase in PBF, it would be interesting to determine how the microRNAs are downregulated. One suggestion could be based on epigenetics, whereby DNA methylation causes a silencing of the genes that microRNAs are transcribed from. This phenomenon has been observed previously with respect to miR-124 gene promoters in an aggressive breast cancer cell line, where hypermethylation resulted in the decreased expression of miR-124 (Lv, X.B., et al., 2011). However, this was shown to be partially reversed by a DNA demethylating agent (Lv, X.B., et al., 2011) highlighting potential clinical relevance in restoring microRNA deregulation.

Alternatively, due to previous studies suggesting that a re-introduction of specific microRNAs underexpressed in cancer cells may benefit in reversing tumourigenesis (Trang, P., et al., 2009), another avenue of potential clinical relevance that could be investigated is the re-introduction of hsa-miR-122-5p, hsa-miR-124-3p or hsa-miR-506-3p into a system. It could then be observed whether PBF overexpression is decreased and consequently, whether there is a benefit in thyroid cancer prognosis. To assess this, an already established murine model could be used, whereby nude mice are injected with NIH-3T3 cells stably expressing PBF, which causes the subsequent growth of aggressive tumours (Stratford, A.L., et al., 2005). Following this, administration of hsa-miR-122-5p, hsa-miR-124-3p or hsa-miR-506-3p mimics respectively to the nude mice would allow determination of whether there is an improvement within these mice compared to those treated with a negative control. In addition, further investigations could be completed by isolating RNA from normal and cancerous tissue and completing qRT-PCR to determine whether there is also a reduction in PBF upon

microRNA administration. If these *in vivo* studies did show a decrease in PBF and a subsequent phenotypic benefit, the application to humans could be extended.

#### **4.5. Conclusion**

Results indicated hsa-miR-122-5p decreased PBF protein significantly at 25kDa in SW1736 cells although; this decrease was not reflected in PBF mRNA expression. Furthermore, hsa-miR-124-3p and hsa-miR-506-3p decreased PBF mRNA expression as well as PBF protein levels at 25kDa in SW1736 cells, albeit non-significantly. Due to limitations within this investigation, these preliminary findings of hsa-miR-122-5p, hsa-miR-124-3p and hsa-miR-506-3p targeting PBF would need to be confirmed by optimising conditions and repeating these experiments.

If these microRNAs were confirmed to target PBF, it would suggest a mechanism of PBF regulation whereby upon specific microRNA deregulation an overexpression of PBF is caused, resulting in thyroid tumourigenesis. Due to the emerging importance of microRNAs as biomarkers and therapeutics the identification of specific microRNAs that play a role in thyroid tumourigenesis may be clinically relevant.

## 5. REFERENCES

- Abraham, D., et al., 2011. MicroRNA Profiling of Sporadic and Hereditary Medullary Thyroid Cancer Identifies Predictors of Nodal Metastasis, Prognosis and Potential Therapeutic Targets. *Clinical Cancer Research*, 17, pp.4772-4781.
- Arora, H., et al., 2013. MiR-506 Regulates Epithelial Mesenchymal Transition in Breast Cancer Cell Lines. *PLoS ONE*, 8, pp.1-7.
- Bentwich, I., 2005. Prediction and Validation of MicroRNAs and their Targets. *RNAi: Mechanisms, Biology and Applications*, 579, pp.5904-5910.
- Bhaijee, F. and Nikiforov, Y.E., 2011. Molecular Analysis of Thyroid Tumors. *Endocrine Pathology*, 22, pp.126-133.
- Boelaert, K., et al., 2007. PTTG and PBF Represses the Human Sodium Iodide Symporter. *Oncogene*, 26, pp.4344-4356.
- Cai, X., et al., 2004. Human MicroRNAs are Processed from Capped, Polyadenylated Transcripts That Can Also Function as mRNAs. *RNA*, 10, pp.1957-1966.
- Cannell, I.G., et al., 2008. How do microRNAs Regulate Gene Expression. *Biochemical Society Transactions*, 36, pp.1224-1231.
- Carther, R.W., 2006. Gene Regulation by MicroRNAs. *Current Opinion in Genetics and Development*, 16, pp.203-208.
- Chien, W. and Pei, L., 2000. A Novel Binding Factor Facilitates Nuclear Translocation and Transcriptional Activation Function of the Pituitary Tumor-transforming Gene Product. *The Journal of Biological Chemistry*, 275, pp.19422-19427.
- Dvořáková, S., et al., 2014. Hereditary Thyroid Carcinoma and its Molecular Diagnostics. *Cesk Patol*, 50, pp.81-86.
- Dweep, H., et al., 2011. MiRWalk – Database: Prediction of Possible miRNA Binding Sites by ‘Walking’ the Genes of Three Genomes. *Journal of Biomedical Informatics*, 44, pp.839-47. (MiRWalk website: <http://www.umm.uni-heidelberg.de/apps/zmf/mirwalk/genetarget.html> accessed on 30/10/13).
- Friedman, R.C., et al., 2009. Most Mammalian mRNAs Are Conserved Targets of MicroRNAs. *Genome Research*, 19, pp.92-105. (TargetScan website: <http://www.targetscan.org/> accessed on 30/10/13).
- Guo, H., 2010. Mammalian MicroRNAs Predominantly Act to Decrease Target mRNA Levels. *Nature*, 466, pp.835-841.

- Hsu, S.D., et al., 2010. MiRTarBase: a Database Curates Experimentally Validated MicroRNA–Target Interactions. *Nucleic Acids Research*, pp.1-7. (MiRTarBase website: <http://mirtarbase.mbc.nctu.edu.tw/> accessed on 30/10/13).
- Hsueh, C., et al., 2013. Prognostic Significance of Pituitary Tumor-Transforming Gene-Binding Factor (PBF) Expression in Papillary Thyroid Carcinoma, *Clinical Endocrinology*, 78, pp.303-309.
- Jacques, C., et al., 2013. DNA Microarray and miRNA Analyses Reinforce the Classification of Follicular Thyroid Tumours. *The Journal of Clinical Endocrinology & Metabolism*, 98, pp.E981-E989.
- Kawamata, T., et al., 2011. Multilayer Checkpoints for MicroRNA Authenticity During RISC Assembly. *EMBO*, 12, pp.944-949.
- Lee, Y., et al., 2004. MicroRNA Genes are Transcribed by RNA Polymerase II. *EMBO*, 23, pp.4051-4060.
- Leivonen, S-K., et al., 2011. Identification of miR-193b Targets in Breast Cancer Cells and Systems Biological Analysis of Their Functional Impact. *Molecular and Cellular Proteomics*, 10, pp.1-9.
- Leone, V., et al., 2011. MiR-1 is a Tumour Suppressor in Thyroid Carcinogenesis Targeting CCND2, CXCR4, and SDF-1 $\alpha$ . *The Journal of Clinical Endocrinology & Metabolism*, 96, pp.E1388-E1389.
- Leonardi, G.C., et al., 2012. MicroRNAs and Thyroid Cancer: Biological and Clinical Significance (Review). *International Journal of Molecular Medicine*, 30, pp.991-999.
- Li, C., et al., 2012. Hepatitis B Virus mRNA-Mediated miR-122 Inhibition Upregulates PTTG1-Binding Protein, Which Promotes Hepatocellular Carcinoma Tumour Growth and Cell Invasion. *Journal of Virology*, 87, pp.2193-2205.
- Lim, S.M., et al., 2012. Treatment Outcome of Patients with Anaplastic Thyroid Cancer: A Single Center Experience. *Yonsei Medical Journal*, 53, pp.352-357.
- Liu, J., et al., 2005. MicroRNA-Dependent Localisation of Targeted mRNAs to Mammalian P-bodies. *Nature Cell Biology*, 7, pp.719-723.
- Lv, X.B., et al., 2011. MiR-124 Suppresses Multiple Steps of Breast Cancer Metastasis by Targeting a Cohort of Pro-Metastatic Genes In Vitro. *Chinese Journal of Cancer*, 30, pp.821-830.
- MacFarlane, L.A. and Murphy, P.R., 2010. MicroRNA: Biogenesis, Function and Role in Cancer. *Current Genomics*, 11, pp.537-561.

- Mazzaferri, E.L. and Kloos, R.T., 2001. Current Approaches to Primary Therapy for Papillary and Follicular Thyroid Cancer. *The Journal of Clinical Endocrinology & Metabolism*, 86, pp.1447-1463.
- Nikiforova, M.N., et al., 2009. MicroRNA Expression Profiles in Thyroid Tumors. *Endocrine Pathology*, 20, pp.85-91.
- Read, M.L., et al., 2011. Proto-Oncogene PBF/PTTG1IP Regulates Thyroid Cell Growth and Represses Radioiodide Treatment. *Cancer Research*, 71, pp.6153-6164.
- Read, M.L., et al., 2014. The PTTG1-Binding Factor (PBF/PTTG1IP) Regulates p53 Activity in Thyroid Cells. *Endocrinology*, 155, pp.1222-1234.
- Ricci, E.P., et al., 2011. Activation of a MicroRNA Response in trans Reveals a New Role for Poly(A) in Translational Repression. *Nucleic Acids Research*, 39, pp.5215-5231.
- Sharma, N., et al., 2012. PBF Interacts with Cortactin and Thyroglobulin in Thyroid Cells. *Endocrine Abstracts*, 28, p.338.
- Smith V. and McCabe C., 2008. PTTG1IP (Pituitary Tumor-Transforming 1 Interacting Protein). *Atlas of Genetics and Cytogenetics in Oncology and Haematology*. (Webpage: <http://AtlasGeneticsOncology.org/Genes/PTTG1IPID41944ch21q22.html> Accessed on 27/12/13).
- Smith, V.E., et al., 2011. Expression and Function of the Novel Proto-Oncogene PBF in Thyroid Cancer: A New Target for Augmenting Radioiodine Uptake. *Journal of Endocrinology*, 210, pp.157-163.
- Smith, V.E., et al., 2013. Manipulation of PBF/PTTG1IP Phosphorylation Status; a Potential New Therapeutic Strategy for Improving Radioiodine Uptake in Thyroid and Other Tumors. *The Journal of Clinical Endocrinology & Metabolism*, 98, pp.2876-2886.
- Stratford, A.L., et al., 2005. Pituitary Tumor Transforming Gene Binding Factor: A Novel Transforming Gene in Thyroid Tumorigenesis. *The Journal of Clinical Endocrinology & Metabolism*, 90, pp.4341–4349.
- Trang, P., et al., 2009. MicroRNAs as Potential Cancer Therapeutics. *Oncogene*, 27, pp.S52-S57.
- Tuttle, R.M., 2013. Differentiated Thyroid Cancer: Overview of Management. UpToDate. (Webpage: <http://www.uptodate.com/contents/differentiated-thyroid-cancer-overview-of-management#H4610264> Accessed on 07/05/14).
- Visone, R., et al., 2007. Specific MicroRNAs are Downregulated in Human Thyroid Anaplastic Carcinomas. *Oncogene*, 26, pp.7590-7595.

Vriens, M.R., et al., 2012. MicroRNA Expression Profiling is a Potential Diagnostic Tool for Thyroid Cancer. *Cancer*, 118, pp.3426-32.

Wang, B., et al., 2012. MiR-122 Inhibits Cell Proliferation and Tumorigenesis of Breast Cancer by Targeting IGF1R. *PLoS ONE*, 7, pp.1-9.

Wang, X., 2008. MiRDB: a MicroRNA Target Prediction and Functional Annotation Database with a Wiki Interface. *RNA*, 14, pp. 1012-1017. (MiRDB website: <http://mirdb.org/miRDB/> accessed on 25/10/13).

Wang, X. and El Naga, I.M., 2008. Prediction of Both Conserved and Non-Conserved microRNA targets in Animals. *Bioinformatics*, 24, pp.325-332. (MiRDB website: <http://mirdb.org/miRDB/> accessed on 25/10/13).

Watkins, R.J., et al., 2010. Pituitary Tumor Transforming Gene Binding Factor: A New Gene in Breast Cancer. *Cancer Research*, 70, pp.3739-3749.

Xu, X., et al., 2013. Micro-RNA-124-3p Inhibits Cell Migration and Invasion in Bladder Cancer Cells by Targeting ROCK1. *Journal of Translational Medicine*, 11.

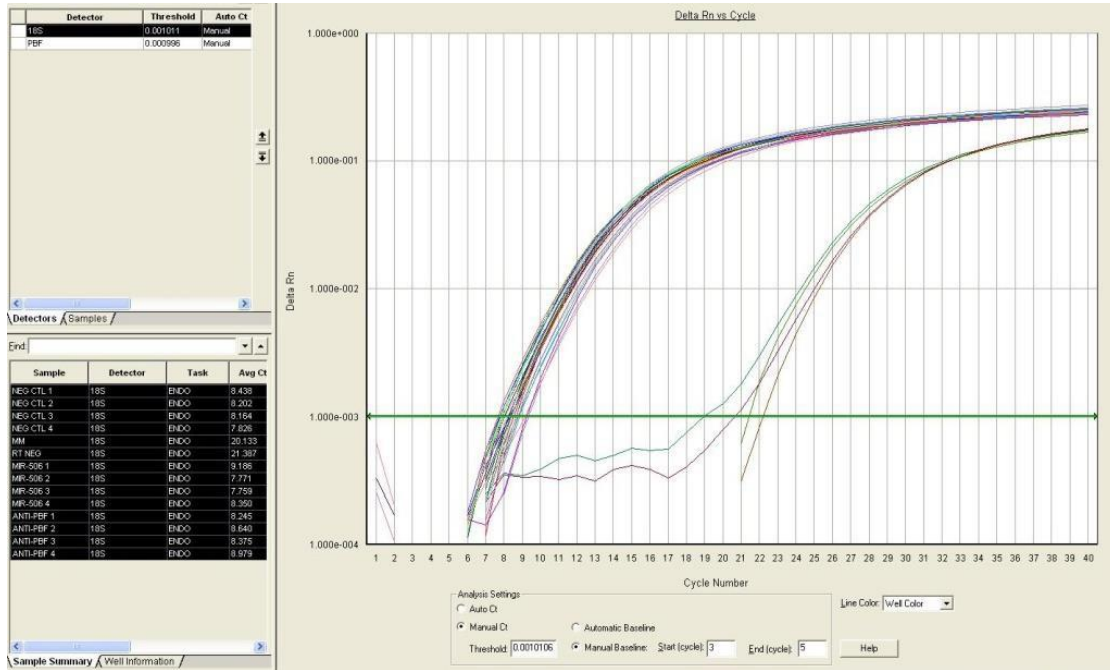
Yi, R., et al., 2003. Exportin-5 Mediates the Nuclear Export of Pre-MicroRNAs and Short Hairpin RNAs. *Genes & Development*, 17, pp.3011-3016.

Yoshimoto, N., et al., 2011. Distinct Expressions of microRNAs that Directly Target Estrogen Receptor  $\alpha$  in Human Breast Cancer. *Breast Cancer Research and Treatment*, 130, pp.331-339.

<http://www.cancerresearchuk.org/cancer-help/type/thyroid-cancer/about/thyroid-cancer-risks-and-causes> Accessed on 06/12/13.

## 6. APPENDIX

B



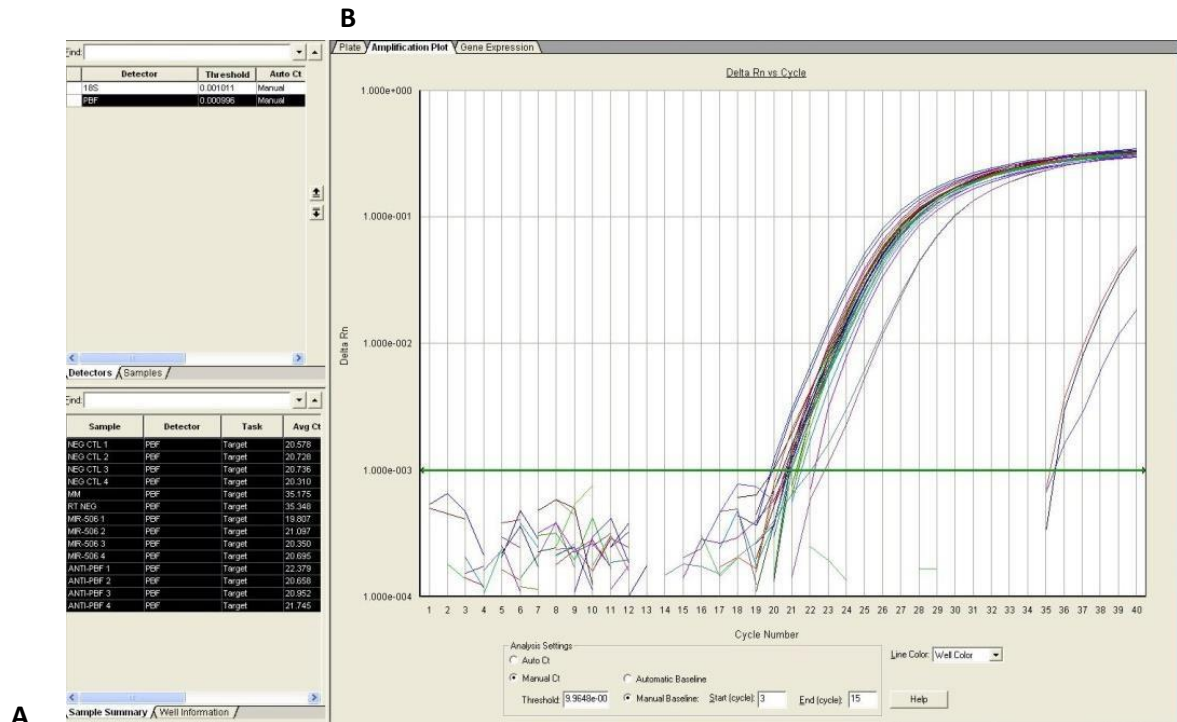
A

**Supplementary figure 1: 18s example plot from 7500 system software**

**A)** Raw data from 7500 system software indicating cDNA and RT negative mastermix controls were at higher average CT values compared to data from samples containing cDNA and RT positive mastermix.

**B)** Plots for 18s for samples containing cDNA and RT positive mastermix can be seen close together with cDNA and RT negative mastermix control plots at a higher cycle number. The threshold bar can be seen at 1.000e-003 Delta Rn.





**Supplementary figure 2: PBF example plot from 7500 system software**

**A)** Raw data from 7500 system software indicating cDNA and RT negative mastermix controls were at higher average CT values compared to data from samples containing cDNA and RT positive mastermix.

**B)** Plots for PBF for samples containing cDNA and RT positive mastermix can be seen close together with cDNA and RT negative mastermix control plots at a higher cycle number. The threshold bar can be seen at 1.000e-003 Delta Rn.

